H. J. Hall

TECHNICAL REPORT

WVT-RI-6216

FATIGUE CHARACTERISTICS OF OPEN-END THICK-WALLED CYLINDERS UNDER CYCLIC INTERNAL PRESSURE

BY

T. E. DAVIDSON

R. EISENSTADT

A. N. REINER

AUGUST 1962

WVT-RI-6216

U.S. ARMY WEAPONS COMMAND

WATERVLIET ARSENAL

RESEARCH & ENGINEERING DIVISION

WATERVLIET NEW YORK

NICAL REPORT

WVT-RI-6216

CHARACTERISTICS OF OPEN-END THICK-WALLED NDERS UNDER CYCLIC INTERNAL PRESSURE

BY
T. E. DAVIDSON
R. EISENSTADT
A. N. REINER

AUGUST 1962

ARMY WEAPONS COMMAND
ERVLIET ARSENAL
RCH & ENGINEERING DIVISION
ATERVLIET NEW YORK

DISPOSITION

This report will be destroyed by the holder when no longer required.

ADDITIONAL COPIES

Qualified requesters may obtain copies of this report from ASTIA.

Copies available at Office of Technical Services $1.25.

The findings in this report are not to be construed as an official Department of the Army position.

FATIGUE CHARACTERISTICS OF OPEN-END THICK-WALLED CYLINDERS UNDER CYCLIC INTERNAL PRESSURE

Abstract

Thick-walled cylinder fatigue data due to cyclic internal pressure for open-end cylinders in the range of 10^3 to 10^5 cycles to failure and having a diameter ratio of 1.4 to 2.0 at a nominal yield strength of 160,000 pounds per square inch is presented. Discussed and also presented are the effects of autofrettage on the fatigue characteristics of thick-walled cylinders. Autofrettage substantially enhances fatigue characteristics at stress levels below the corresponding overstrain pressure; the degree of improvement increasing with decreasing stress levels. The rate of improvement in fatigue characteristics increases significantly with diameter ratio in autofrettaged cylinders up to a diameter ratio of 1.8 - 2.0 and to a much smaller degree in the non-autofrettaged condition. The rate of improvement of fatigue characteristics above 2.0 is the same for both the autofrettaged and non-autofrettaged cases.

It is shown that thermal treatment of 675°F for 6 hours after autofrettage does not affect fatigue characteristics and that there is a correlation between the cyclic stress level and the area and depth of the fatigue crack to the point of ductile rupture. The depth of the fatigue crack decreases with increasing cyclic stress level.

A means for using data from a uni-directional tensile fatigue test to predict the fatigue characteristics of thick-walled cylinders is discussed.

Cross-Reference Data

Fatigue
Fracture
Gun Barrels
Pressure Vessel
Thick-Walled Cylinders

CONCLUSIONS

Data for the hydrostatic fatigue characteristics of high-strength, thick-walled cylinders in the range of 10^3 to 10^5 cycles to failure are presented. Based on this investigation, the following points have been established:

1. Autofrettage significantly improves the fatigue characteristics of thick-walled cylinders at stress levels lower than those associated with the overstrain pressure. The degree of improvement increases as the cyclic stress level decreases.
2. Using the difference in principal bore stress as the cyclic paramater, the fatigue characteristics improve with increasing diameter ratio. This increase with diameter ratio is small in the case of the non-autofrettaged condition. In the case of autofrettaged cylinders, the increase in fatigue life with diameter ratio is substantial. The rate of improvement in the autofrettaged cylinders approaches that for the non-autofrettaged condition beyond a diameter ratio of 2.0.
3. The slope of the difference in principal bore stress versus cycles to failure curve appears to approach zero below 10^3 cycles to failure.
4. Based on the similarity in the correlation coefficient, no single cyclic stress or strain parameter evaluated for the presentation of thick-walled cylinder fatigue data offered significant advantage over the others.
5. Thermal treatment of the overstrained cylinders at 675°F for 6 hours did not affect fatigue characteristics.
6. There is a correlation between the cyclic stress level and the area and depth of the fatigue crack to the point of ductile rupture; the depth of the crack decreasing with increasing stress level.
7. Internal diameter surface finishes varying from 16 to .125 micro-inches RMS did not show a consistent pattern in affecting the fatigue life.

T. E. Davidson
T. E. DAVIDSON

R. Eisenstadt
R. EISENSTADT

A. N. Reiner
A. N. REINER

Approved:

R. E. Weigle
R. E. Weigle
Chief Scientist

L. J. Wooge
L. J. Wooge
Capt., Ord Corps
Chief, Research and Engineering Division

TABLE OF CONTENTS

FIGURES

TABLE

LIST OF SYMBOLS

σ	Stress in pounds per square inch
Y.S.	Yield strength, pounds per square inch
U.T.S.	Ultimate tensile strength, pounds per square inch
E	Modulus of elasticity, pounds per square inch
ν	Poisson's Ratio
P	Test pressure, pounds per square inch
b	Outside diameter of cylinder, - inches
a	Inside diameter of cylinder, - inches
W	Wall ratio b/a
NA	Non-Autofrettaged
A	Autofrettaged
D	Ratio of lower limit of the 99.9% confidence level to least squares value
N	Cycles to Failure
R	Radius of elastic-plastic interface, - inches
t	Confidence level coefficient
S	Standard deviation
x	Logarithm to base 10 of cycles to failure
n	Number of experimental points
d	Depth of crack, - inches
r	Correlation coefficient
w	Wall thickness, - inches

SUBSCRIPTS

$( )_t$	Tangential
$( )_r$	Radial
$( )_z$	Longitudinal
$( )_y$	Yield
$( )_p$	Plastic
$( )_{trp}$	Tangential residual plastic
$( )_{rrp}$	Radial residual plastic
$( )_c$	Confidence level
$(\bar{})$	Least squares value of function

INTRODUCTION

The current trend is towards the design of pressure vessels for use at higher operating stress levels. One of the most common techniques for extending the elastic load carrying capacity is by autofrettage. For example, the operating pressure to weight ratio for cannon type weapons has been substantially increased in recent years by the combined use of high-strength materials and autofrettage. Similar advances have been made in other areas where the requirement exists for vessels capable of operating at very high pressures.

In many instances, the operation of highly stressed pressure vessels is cyclic in nature. In these instances, it is not enough to consider the yielding characteristics alone, but one must also take into account the problem of fatigure life and the manner in which it is affected by such techniques as autofrettage for increasing elastic load carrying capacity. This report summarizes the results of an experimental program aimed at the study of the fatigue characteristics of high-strength open-end cylinders of intermediate diameter ratio.

The fatigue characteristics of closed-end cylinder cyclically stressed in the region of the endurance limit has been reported by Morrison[1]. He has found that, in the region of the endurance limit, the residual stresses associated with overstrain substantially enhances fatigue life. Similar results were found by Newhall and Kosting[2] for several rifled sections of cannon tubes, at somewhat higher stress levels.

In light of the current interest in the use of highly stressed pressure vessels, the investigation to be described herein involves a study of fatigue characteristics of thick-walled cylinders in what is commonly referred to as the low cycle fatigue range, that is, up to approximately 10^5 cycles to failure. Presented are data for open-end cylinders in the diameter ratio range of 1.4 to 2.0 at a nominal yield strength level of 160,000 pounds per square inch. Data is also presented on the effects of autofrettage on fatigue characteristics as a function of diameter ratio and cyclic stress level. The possibility of utilizing a simple tensile fatigue test to predict the life of thick-walled cylinders, and the mode of fatigue fracture for cylinders exposed to cyclic internal pressures is discussed.

PROCEDURE

Test Specimens

The specimens utilized in this program consisted of a common one-inch internal diameter and diameter ratios of 1.4, 1.6, 1.8 and 2.0.

The specimen material was of a 4340 type composition with the following nominal chemical analysis in percent:

Carbon	0.37	Nickel	2.39
Manganese	0.72	Chromium	0.98
Silicon	0.28	Molybdenum	0.38
Sulphur	0.035	Phosphorous	0.016

Specimens were heat-treated to a nominal yield strength of 160,000 pounds per square inch by austenizing at 1525°F; oil quenching, and tempering at 1075°F ± 25°. Tensile and Charpy test specimens were taken from each group of three specimens which were heat-treated in 40-inch lengths.

After heat treatment, sufficient material was removed from the bore to eliminate any decarburization. The final surface finish on the internal diameter ranged from 16 to 125 RMS.

The autofrettaged specimens were overstrained 100 percent in the manner described in reference (3). Those specimens that were thermally treated after autofrettage to reduce anelastic effects were subjected to a temperature of 675°F for 6 hours.

Test Apparatus

The pressure systems used in this program consisted of two basic types. The first type is a Harwood Engineering Company system of 80,000 pounds per square inch capacity with a cyclic rate of up to 20 cycles/minute. As shown in figure (1), the pressure source consists of an intensifier-type pump which feeds high-pressure fluid into the specimens through a manifold shown in figure (2). As can be noted, four specimens may be tested simultaneously. The holding press serves to support the pressure packings which effectively eliminates longitudinal forces in the specimen; thus, resulting in the open-end condition for the specimens. Upon attaining the peak pressure, a valve is opened and the pressure dropped to near atmospheric level. The high-pressure fluid is an instrument oil. A schematic of this system is shown in figure (3).

The second type is a Harwood Engineering Company system of 150,000 pounds per square inch capacity with a cyclic rate of up to 10 cycles/minute. As shown in figure (4), it also consists of an intensifier-type pumping system which feeds pressure into the specimens. In contrast to the former system, the pressure is released by removing the drive pressure in the intensifier instead of venting to atmosphere; thus, resulting in a closed system. This results in the pressure not returning to zero between cycles, but to a value of approximately 2,500 pounds per square inch. However, since this system is used primarily above 80,000 pounds per square inch, a small residual pressure will have little effect, and the comparative results from both systems are in the range of anticipated experimental error. A schematic of this system is shown in figure (5).

Instrumentation

Pressure Control and Recording

In the 80,000 pounds per square inch system, pressure measurement is by means of Manganin wire-type pressure transducers. Two such transducers are used. One serves as input to the "Rotax" control unit which regulates the automatic cycling of the pressure system through a self-balancing "servo" system equipped with electrical contacts and recording pen. The setting of control contacts relative to the desired indicated pressure determines the point of opening and closing of the dump valve as well as stopping the main intensifier at the end of each pressure peak. The second transducer is used to monitor and record the total pressure cycle on an oscillographic recorder.

The second basic type of pressure transducer, known as a bulk modulus cell, is used in the 150,000 pounds per square inch system. It is a mechanical device designed to sense the linear motion produced by a cylinder with one end closed and exposed to the pressure being measured. This particular system uses a low-pressure air transmitter and receiver unit to remotely record and control peak and minimum specimen pressure.

The error in the measurement and recording of pressure is estimated to be approximately one percent in the calibration of the pressure transducer and two percent in the recording system due to the cyclic conditions.

Strain Measurement and Recording

To insure that each specimen is at the anticipated test pressure, two strain gages are mounted diametrically opposite each other at the mid-length of each specimen. The output of one gage on each specimen is monitored on an oscillographic recorder. In normal operation the instruments are set to record the full elastic strain cycle. The recording system, along with the control panel for the 150,000 pounds per square inch system, is shown in figure (6).

THEORY

Fatigue failure can be divided into two phases. The first phase consists of the microscopic initiation of the crack. The second stage consists of the propagation of the fatigue crack to the point where the specimen or component can no longer support the applied cyclic load and failure occurs. To a great extent, this second stage is dependent upon the applied tensile stress and; therefore, would be affected by superimposed mean or residual stresses and stress gradients. It is this second stage that will be of primary concern in this paper.

It is well-known that a compressive mean stress increases the allowable cyclic stress amplitude for a given fatigue life. Conversely, a mean tensile stress decreases the allowable amplitude stress as shown in the following diagram from H. Sigwart[4] where σ_m is the mean and σ the cyclic stress.

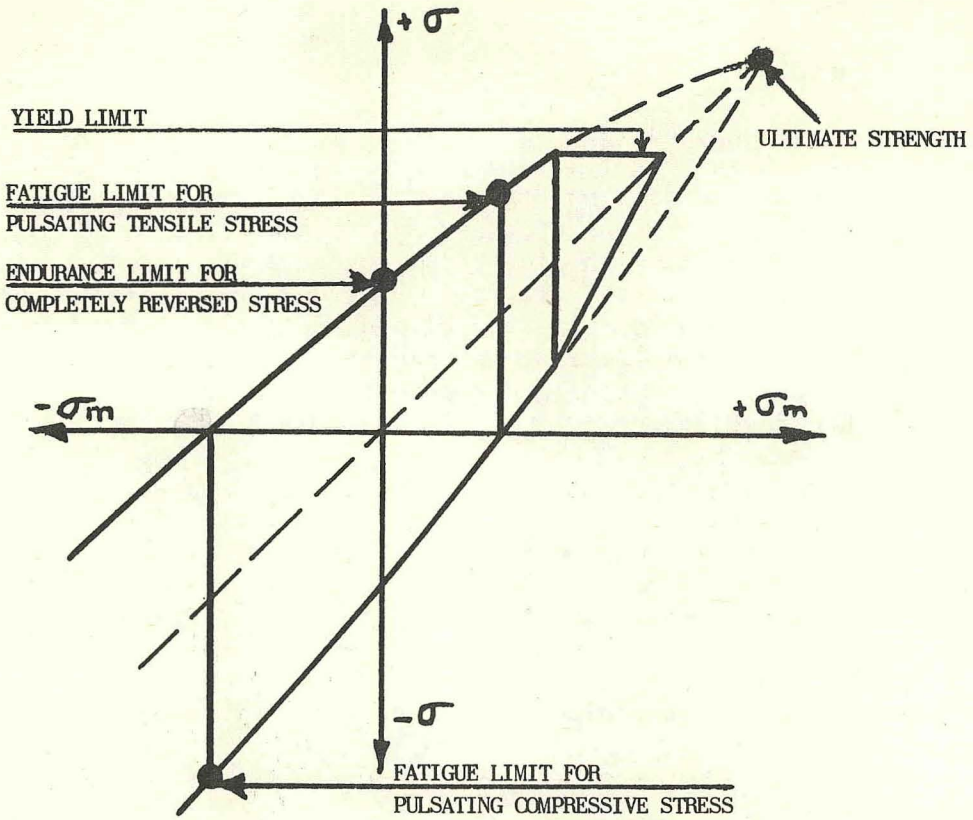

In an overstrained thick-walled cylinder, the tangential and radial residual stress distribution is described by the relationships[3] based on the Tresca yield criterion:

$$\sigma_{trp} = \frac{\sigma_y}{2}\left[\frac{b^2 + R^2}{b^2} + 2\log\frac{r}{R} - \frac{a^2}{b^2 - a^2}\left(\frac{b^2 - R^2}{b^2} + 2\log\frac{R}{a}\right)\left(1 + \frac{b^2}{r^2}\right)\right] \quad (1)$$

and

$$\sigma_{rrp} = \frac{\sigma_y}{2}\left[\frac{b^2 - R^2}{b^2} + 2\log\frac{r}{R} - \frac{a^2}{b^2 - a^2}\left(\frac{b^2 - R^2}{b^2} + 2\log\frac{R}{a}\right)\left(1 - \frac{b^2}{r^2}\right)\right] \quad (2)$$

For the 100 percent overstrain condition, i.e., R = b, these relationships become:

$$\sigma_{trp} = \frac{\sigma_y}{2}\left[2 + 2\log\frac{r}{b} - \frac{a^2}{b^2 - a^2}\left(2\log\frac{b}{a}\right)\left(1 + \frac{b^2}{r^2}\right)\right] \quad \ldots\ldots (3)$$

and

$$\sigma_{rrp} = \frac{\sigma_y}{2}\left[2\log\frac{r}{b} - \frac{a^2}{b^2 - a^2}\left(2\log\frac{b}{a}\right)\left(1 - \frac{b^2}{r^2}\right)\right] \quad \ldots\ldots (4)$$

Equations (3) and (4) are shown in figure (7) for a 2.0 diameter ratio in the 100 percent overstrain condition. As can be seen, the tangential residual stress is compressive at the bore.

In view of the compressive residual stress, it would be expected that the overstrained, or autofrettaged, cylinder will withstand a higher cyclic pressure for a given life or a longer life for a given stress level than the non-autofrettaged cylinder. Since, for the 100 percent overstrain condition, the magnitude of the residual stresses increases with diameter ratio, it would also be expected that the increased life due to autofrettage would also increase with diameter ratio.

By equating the tangential residual stress to the yield strength of the material in compression, it is found for the 100 percent overstrain condition; assuming the simplified maximum shear stress yield criterion, that beyond a diameter ratio of approximately 2.2, the cylinder will reverse yield upon the release of the overstrain pressure. Theoretically then, the increase in fatigue characteristics due to autofrettage will approach a maximum at the 2.2 diameter ratio level. As will be shown however, due to what appears to be the Bauschinger effect, this critical diameter ratio appears to be in the range of 1.8 - 2.0 instead of 2.2.

RESULTS AND DISCUSSION

Analysis of Various Cyclic Parameters for Use in Presenting Fatigue Data

In the presentation of fatigue data for thick-walled cylinders, several cyclic parameters may be plotted against life in terms of number of cycles of failure. How the fatigue data for the non-autofrettaged cylinders appears when plotted in terms of various cyclic parameters is shown in figures 8 through 12. For simplicity in comparing the various cyclic parameters, only the least squares line for each diameter ratio corresponding to the regression of the cycles to failure on the pressure or stress level along with the correlation coefficient (equation 6) for all of the data in terms of the pertinent cyclic parameter will be shown in this series of figures.

Based on conventional statistical theory, the general relationship describing the least squares line for the regression of x on y is:

$$x = a + b\,(y - \bar{y}) \qquad \ldots\ldots\ldots\ldots\ldots\ldots\ldots\ldots\ldots\ldots \quad (5)$$

where for the purposes of this investigation

$$y = \log\,(\text{cyclic parameter})$$

$$a = \bar{y} = \frac{\sum y}{n}$$

$$x = \frac{\sum x}{n} = \frac{\sum \log\,(\text{No. cycles to failure})}{n} \quad \text{and}$$

$$b = \frac{\sum (x - \bar{x})\quad (y - \bar{y})}{\sum (y - \bar{y})^2}$$

The correlation coefficient (r) is defined by

$$r = \frac{\sum (x - \bar{x})\quad (y - \bar{y})}{\sqrt{\sum (x - \bar{x})^2\quad (y - \bar{y})^2}} \qquad \ldots\ldots\ldots\ldots\ldots\ldots \quad (6)$$

and is a measure of the effectiveness or probability of the data being described by the defined least squares line and, as will be shown, is an indication of the relative data spread for the various cyclic parameters.

The data could also be statistically analyzed in terms of the regression of y on x. However, because of the high correlation coefficients of the experimental results, varying from .91 to .986, there are only minor variations between the regressions, and only one will be shown.

For the purpose of minimizing the effects of minor property variations in the test specimens, and to enable comparison of the results of this work with those of other investigators, all cyclic parameters and the data presented herein will be normalized with respect to the ultimate tensile strength, except where otherwise specified.

In the simplest form, the data may be plotted as cyclic pressure versus cycles to failure, as shown in figure 8, for a series of non-autofrettaged cylinders. As can be noted, there are distinctive lines corresponding to each individual diameter ratio. This would be expected since the maximum tangential stress for any given pressure decreases with increased diameter ratio.

Figure 9 for the same data shows normalized maximum tangential stress at the bore which is defined as

$$\frac{\sigma_t}{UTS} = \frac{P}{UTS}\,\frac{W^2 + 1}{W^2 - 1} \qquad \ldots\ldots\ldots\ldots\ldots\ldots\ldots\ldots \quad (7)$$

as a function of cycles to failure. As would be expected, a large amount of the diameter ratio dependence has been removed. It should be noted; however, that the least squares line for the smaller diameter ratio is at

a higher value than the larger diameter ratio. This is opposite to what would be expected. The actual initiation of the fatigue crack can probably be predicted by some cyclic stress or strain parameter independent of diameter ratio. The crack, however, must propagate over a larger area in the larger diameter. Intuitively then, the larger diameter ratio should be at a higher stress and life level. Based on this, fatigue failure is probably some function of a combined stress condition instead of a single principal stress.

Figure 10 shows the difference in the principal stresses at the bore as defined by

$$\frac{\sigma_t - \sigma_r}{UTS} = \frac{2PW^2}{UTS(W^2 - 1)} \quad \ldots\ldots\ldots\ldots\ldots\ldots \quad (8)$$

as a function of the number of cycles to failure. As can be noted, the diameter ratio dependency is again small with the larger diameter ratio logically exhibiting the higher fatigue strength characteristics.

Figure 11 shows the data in terms of the normalized octahedral stress as defined by

$$\frac{1}{UTS}\left\{\left[(\sigma_t - \sigma_r)^2 + (\sigma_r - \sigma_z)^2 + (\sigma_z - \sigma_t)^2\right]\frac{1}{2}\right\}^{\frac{1}{2}} \quad \ldots \quad (9)$$

which, since $\sigma_z = 0$, yields

$$\frac{1}{UTS}\left[\sigma_t^2 + \sigma_r^2 - \sigma_t\sigma_r\right]^{\frac{1}{2}} \quad \ldots\ldots\ldots\ldots\ldots \quad (10)$$

A strain parameter defined by

$$\frac{\sigma_t - \nu\,\sigma_r}{E} \quad \ldots\ldots\ldots\ldots\ldots\ldots\ldots \quad (11)$$

may also be used as shown in figure 12. It should be noted, however, that again, as in the case of σ_t vs. life, as shown in figure 9, the smaller diameter ratios lie above the larger diameter ratios.

As can be noted from the similarity of correlation coefficients which are related to the spread of the data for the various cyclic parameters shown in figures 8 through 12, it makes little difference statistically as to what cyclic stress or strain parameter is chosen to plot the data. The magnitude of the data spread due to diameter ratio dependence is approximately

the same in each case with only the order being different. For the purpose of this report then, all data, unless otherwise specified, will be presented in terms of the normalized difference in principal bore stress as defined by equation (8).

Effects of Autofrettage on Fatigue Life

The effects of autofrettage on fatigue life, as compared to the non-autofrettaged condition, is shown in figures 13, 14, 15 and 16 respectively for the diameter ratios of 1.4, 1.6, 1.8 and 2.0. A compilation of the least squares lines for all diameter ratios in terms of the difference in principal bore stresses and cyclic pressure is shown in figures 17 and 18 respectively.

In the statistical data shown in the legend of these figures, S is the standard deviation as defined by

$$S = \sqrt{(1 - r^2) \quad \frac{\sum (x - \bar{x})^2}{n - 2}} \qquad \ldots\ldots\ldots\ldots\ldots (12)$$

and t_c is the confidence level coefficient for a two-sided normal distribution which depends on the confidence level and the degrees of freedom defined as the number of test points minus two. In the figures, the values of t shown are for 99.9 percent and 99.0 percent confidence level. Coefficients for other confidence levels can be obtained from standard texts on statistics dealing with the treatment of experimental data [5] [6].

The limits for a given confidence band are closely approximated by the following relationship where $\bar{x}$ is in $\log_{10}$

$$x_c = \bar{x} \pm t_c S \qquad \ldots\ldots\ldots\ldots\ldots\ldots\ldots (13)$$

which represents a straight line parallel to the least squares line on the curves presented. The relationship of cycles to failure to x is

$$N = (10^{x_c}) \qquad \ldots\ldots\ldots\ldots\ldots\ldots\ldots (14)$$

For simplicity in using these curves, the value of D_c shown in the legend, is the ratio of cycles to failure for the lower limit of confidence level indicated to the least squares value at a particular stress or pressure level. For example, the lower limit of life with 99.95 percent confidence is given by the relation

$$N_{99.95} = \bar{N} D_{99.9} \qquad \ldots\ldots\ldots\ldots\ldots\ldots (15)$$

As can be seen in the above-mentioned figures, there is an improvement in the fatigue characteristics of autofrettaged cylinders as compared to the non-autofrettaged condition. The relative benefit increases with decreasing operating stress level and increasing diameter ratio. The increase in life of the autofrettaged cylinders over the non-autofrettaged condition for several stress levels is summarized in figure (19). For example, considering the case of 2.0 diameter ratio operating at a normalized difference in principal stress of 0.9, which is approximately 10 percent below the elastic breakdown condition, as predicted by the Von Mises yield criterion, the increase in life is a factor of 3.6. Proportional benefits are obtained in the allowable operating stresses to cause failure. Considering the same example, as above, for a life of 50,000 cycles, the average operating stress level, as a result of autofrettage, may be increased 50 percent over that for the non-autofrettaged condition.

Figure 20 is a plot of diameter ratio versus cycles to failure for several differences in principal stress levels. As can be seen, there is a slight diameter ratio dependency for the non-autofrettaged cylinders which is attributed primarily to the greater distance over which the crack must propagate as the diameter ratio increases, before ductile rupture occurs. It is readily seen, however, that the autofrettaged cylinders exhibit a very substantial diameter ratio dependency with the benefit from autofrettage increasing with increased diameter ratio. From equation (3) this would be expected since the magnitude of the compressive residual bore stress increases with diameter ratio. In the region of 1.8 to 2.0 diameter ratio, the slope of the diameter ratio versus cycles to failure curve changes for the autofrettaged condition and approaches that characteristic of the non-autofrettaged cylinders. This indicates that the magnitude of the residual stresses are no longer increasing. However, by equating equation (3) to the yield strength of the material in compression, which is usually assumed substantially equal to that in tension, it can be shown that the maximum residual stress is obtained at a diameter ratio of 2.2, based on the Tresca yield criterion. To some extent this early change in slope is attributed to the Bauschinger effect which from associated work will be reported at a later date, appears to occur at the 2.0 diameter ratio or less for the 100 percent overstrain condition. The Bauschinger effect results in a lowering of the compressive yield strength which in the case of an overstrained thick-walled cylinder, limits the maximum level of the compressive residual bore stress beyond which the cylinder will yield in compression. Beyond the 2.0 diameter ratio then, it is anticipated that the slope of the autofrettaged curve will be the same as that for the non-autofrettaged condition.

The study of the fatigue characteristics of thick-walled cylinders directly, as in the manner described herein, has several experimental difficulties, the most significant being attrition of equipment. It would be desirable then to be able to predict the fatigue characteristics of thick-walled cylinders from some simplified fatigue test. One possible approach to this problem will now be discussed.

As the diameter ratio approaches 1, the radial component of the stress approaches 0 with only the tangential stress remaining. As shown in figure 20, the autofrettaged also approaches the non-autofrettaged condition as the diameter ratio decreases with convergence at W = 1. Since there is only one principal stress at the hypothetical case of W = 1, then it may be possible to correlate this condition with a uniaxial tensile fatigue test. To a first approximation, the slopes of the diameter ratio versus cycles to failure curves for the non-autofrettaged condition are reasonably independent of stress level. Therefore, to determine the fatigue characteristics of thick-walled cylinders of a given material over a wide range of stress levels and diameter ratios would require only the running of a series of tensile fatigue tests at different stress levels, and to determine the slope, only one group of cylinders at a given diameter ratio and stress level. Since for the autofrettaged condition the slope of the diameter ratio versus cycles to failure curves is dependent upon cyclic stress level, two groups of thick-walled cylinders at widely different stress levels in conjunction with the tensile fatigue data would be required to establish, to a close approximation, the entire family of curves for a wide range of diameter ratios and stress conditions of the type shown in figure 20, for the open-end condition, that is, $\sigma_z = 0$. The feasibility of this simplified approach will be investigated further.

As the cyclic stress level increases, the benefits from autofrettage decrease, and at stress levels approaching that for the overstrain pressure, there is little benefit. This is to be expected since the non-autofrettaged cylinders at these stress levels will actually permanently deform; thus, being autofrettaged to a certain degree on the first pressure cycle.

It should be noted that the least squares lines shown in all of the figures intersect the ordinate which corresponds to 1,000 cycles at a stress value closely approaching that for the 100 percent overstrain condition, i.e.,

$$\frac{\sigma_t - \sigma_r}{UTS} = \frac{1.08\ \sigma_y\ \ln W}{UTS} \left[\frac{2W^2}{W^2 - 1} \right] \quad \ldots\ldots\ldots\ldots \quad (16)$$

where $1.08\ \sigma_y\ \ln W$ equals the pressure for 100 percent overstrain[3]. If the least squares line were continued to the 1 cycle condition, the stress level would be well in excess of the rupture pressure which, for the material considered herein, is only slightly in excess of the overstrain pressure. Instead of continuing on however, for the cyclic rates considered in this investigation, there is a leveling off in the very low cycle region and the slope of the curve approaches 0 at stress levels in the neighborhood of that associated with the 100 percent overstrain condition. This very low cycle, high-stress region is a subject of current study.

Effect of Thermal Treatment After Autofrettage

It has been found in another current investigation that thermal treating high-strength autofrettaged cylinders at approximately 675°F for

a period of time tends to increase the elastic load carrying capacity. As shown in figure 21; thermal treatment; however, has little effect on fatigue characteristics as is indicated by the overlapping of the thermally and non-thermally treated data for autofrettaged cylinders in the 1.4 to 1.8 diameter ratio range. Except for this figure then, the thermally and non-thermally treated results were not considered separately.

Effect of Surface Finish and Tensile Strength Variations

The internal diameter surface finishes of the specimens utilized in this program varied from approximately 16 to 125 RMS as measured along the longitudinal axis. However, analysis of the data does not indicate any trends towards dependency of the results upon surface finish over the range encountered.

The fatigue characteristics similarly appear to be proportional to the tensile strength level for the range of ultimate tensile strength from 160,000 to 190,000 pounds per square inch.

Comparison of Results with Other Investigations

On figures 13, 14, 15 and 16, the data of other investigators, Morrison[1], Newhall and Kosting[2], are included. In the case of the Newhall and Kosting, data for large open-end cylinders at ultimate tensile strength levels of 115,000 and 154,000 pounds per square inch, the correlation with the data presented herein is excellent. The Morrison data; however, for both the autofrettaged and non-autofrettaged condition, lies substantially above the presented data. In discussing this apparent discrepancy one must consider that there are three substantial differences in the experimental conditions between the two investigations. Whereas Morrison's specimens were tested as closed-end cylinders, the results presented herein considered the open-end condition, i.e., the longitudinal stress is effectively zero. If the third stress is taken into account theoretically by the octahedral stress parameter (equation 9), the variation is slightly reduced. Except by test, one cannot be certain of the magnitude of the effect of this third stress on fatigue. Therefore, the magnitude by which the third principal stress associated with the closed-end condition affects fatigue is the subject of a current investigation. Secondly, Morrison used a cyclic pressure rate of approximately 1,000 cycles per minute as compared to 6 per minute for this investigation. Thirdly, the bore of Morrison's specimens were lapped to a finish of approximately 1 to 4 RMS which could have a pronounced effect in terms of crack initiation. It is difficult to ascertain the magnitude of the contribution of these various differences to the higher fatigue characteristics reported by Morrison. It is most likely; however, that the most important factor is the difference in surface finish. It is interesting to note that the discrepancy is substantially smaller in the case of the autofrettaged data as compared to the non-autofrettaged condition. This is probably due in part to the tendency for the high compressive tangential residual stress to reduce the effectiveness of the rougher bore surface in enhancing crack initiation.

Fracture Analysis

Representative fatigue failures for thick-walled cylinders of 1.4 and 1.8 diameter ratio at low-cyclic and high-cyclic stress levels are shown in figure 22. As can be noted, there are two characteristic zones. The first zone, which appears lighter, has a smooth appearance with conchoidal markings. This zone, sometimes called the zone of decohesion[6], is characteristic of a cyclically propagating fatigue crack. The second and remaining zone has a fibrous texture which is characteristic of static rupture in a ductile thick-walled cylinder.

From a macroscopic standpoint, the fatigue crack evidently propagates to the depth at which the remaining material is no longer able to withstand the internal pressure, and ductile rupture occurs. As would be expected then, there should be a correlation between the cyclic stress and the fatigue fracture area and depth. By examining a large number of fracture surfaces of the specimens associated with this study, it has been found that there is an approximate linear relationship between the cyclic stress parameter and the crack depth divided by the wall thickness as shown in figure 23. Of course, there is scatter due to the experimental difficulty of determining the exact location of the boundary between the fatigue crack and fibrous rupture zone, as well as the statistical nature of fatigue data. The scatter is, however, not so great that the linear correlation cannot be readily detected over a wide range of cyclic stress levels and wall ratios. A similar linear relationship also exists for the cyclic stress parameter versus the crack area divided by the square of the wall thickness.

It should be noted that only the fatigue crack causing final failure was considered in the above plots. Smaller cracks were also noted in several other areas of the specimen. An example of this condition is shown in figure 22 where several smaller fatigue cracks are readily visible.

ACKNOWLEDGEMENT

The authors wish to express their appreciation for the helpful contributions made by Mr. R. A. Petell and his staff for the conduct of the experimental work, Mr. Earl Skelton for his help with the curves, Messrs. D. P. Kendall and M. Pascual for their constructive comments, Mr. P. Loatman for statistical analysis and computer program.

REFERENCES

(1) "The Strength of Thick-Walled Cylinders Subjected to Repeated Internal Pressure", Morrison, Crossland, and Pairy - Paper No. 59-A-167 ASME Transactions

(2) "Progressive Stress Damage and Strength of Centrifugally Cast CW Gun Tubes", D. H. Newhall, P. R. Kosting - 1949, Watertown Arsenal Laboratory 731/281

(3) "The Autofrettage Principle as Applied to High-Strength Light Weight Gun Tubes", T. E. Davidson, C. S. Barton, A. N. Reiner, D. P. Kendall - Technical Report WVT-RI-5907 - Watervliet Arsenal, Watervliet, N. Y.

(4) "Influence of Residual Stresses on the Fatigue Limit", H. Sigwart, Fig. 3.41, Page 273 of the Proceedings of the International Conference on Fatigue of Metals 1956. Published by Institution of Mechanical Engineers

(5) "Metal Fatigue", Sines and Waisman - McGraw-Hill - 1959, pp. 112-141

(6) "Statistical Tables for Biological, Agricultural, and Medical Research", R. A. Fisher and F. Yates, Oliver and Boyd - Table III

(7) "A Comparison of Ductile and Fatigue Fractures", Crussard, Plateau, Tamhankar, Henry & Lajeunesse, p. 593, "Fracture" J. Wiley & Sons 1960

SPECIMEN NO.	STRENGTH (PSI) YIELD	STRENGTH (PSI) TENSILE	DIAMETER RATIO	TEST PRESSURE (PSI)	CYCLES TO FAILURE	FRACTURE AREA (in^2)	FRACTURE DEPTH (in)	AVG. SURFACE FINISH MICRO-IN
				NA - NON-AUTOFRETTAGED				
55A1	152,400	163,200	1.4	20,000	46,700	0.11	.16	40
55A2	152,400	163,200	1.4	20,000	49,800			40
55A3	152,400	163,200	1.4	20,000	55,000			30
39A1	146,300	160,400	1.4	20,000	55,000			25
74A2	153,000	165,000	1.4	30,000	18,900			40
74A3	153,000	165,000	1.4	30,000	13,900	0.09	.16	45
144A2	170,400	178,400	1.4	30,000	7,780	0.12	.14	60
39A2	146,300	160,400	1.4	30,000	20,620			40
88B3	152,100	163,400	1.4	30,000	60,200			80
76A2	161,700	173,300	1.4	30,000	31,300	0.10	.15	50
39A3	146,300	160,400	1.4	40,000	5,140			30
39B1	143,700	158,400	1.4	40,000	5,370			
39B2	143,700	158,400	1.4	40,000	5,430			70
74A1	153,000	165,000	1.4	40,000	5,190			50
86B1	160,900	172,800	1.4	40,000	6,880			90
87B3	156,600	168,000	1.4	40,000	7,030			95
76B3	157,200	168,800	1.4	50,000	1,570			30
75B1	169,900	180,100	1.4	50,000	2,540			50
82B3	160,800	171,200	1.4	50,000	2,870			45
70A2	150,500	167,400	1.4	50,000	2,310	0.05		
46B2	157,800	167,900	1.6	30,000	26,400			
46B3	157,800	167,900	1.6	30,000	31,500	0.20	.25	45
29B2	154,700	162,400	1.6	30,000	17,500			
70B3	165,400	176,400	1.6	30,000	75,000			
82A3	163,100	174,000	1.6	30,000	75,000			
X71B1	173,700	183,500	1.6	40,000	20,000			
X44B3	171,600	181,300	1.6	40,000	18,940			
61B1	161,200	171,100	1.6	40,000	11,690			

SPECIMEN DATA
Sheet 1 of 7

TABLE I

SPECIMEN NO.	STRENGTH (PSI) YIELD	STRENGTH (PSI) TENSILE	DIAMETER RATIO	TEST PRESSURE (PSI)	CYCLES TO FAILURE	FRACTURE AREA (in^2)	FRACTURE DEPTH (in)	AVG. SURFACE FINISH MICRO-IN
				NA - NON-AUTOFRETTAGED				
61B2	161,200	171,100	1.6	40,000	13,230			50
61B3	161,200	171,100	1.6	40,000	13,120			35
29A3	153,500	161,700	1.6	40,000	14,410			40
83A2	153,700	165,900	1.6	40,000	13,410	0.15		20
83B2	159,600	169,700	1.6	40,000	12,610			
69A3	163,200	173,600	1.6	40,000	13,840	0.20	.23	20
X71B1	175,000	184,700	1.6	40,000	12,190			
78B2	164,400	173,300	1.6	40,000	7,070			45
82B3	160,800	171,200	1.6	40,000	12,060	0.05	.09	100
46A1	152,200	163,900	1.6	50,000	11,350			85
46A3	152,200	163,900	1.6	50,000	6,350			65
46B1	157,800	167,900	1.6	50,000	5,830			40
139A2	163,100	174,300	1.6	50,000	7,500			70
85B3	160,200	171,800	1.6	50,000	8,420			100
87A2	150,100	163,900	1.6	50,000	7,700			
68B1	159,700	170,800	1.6	50,000	6,810			35
113A2	163,200	169,800	1.6	50,000	5,380			115
112B2	154,000	167,800	1.6	50,000	7,250			45
82A2	163,100	174,000	1.6	50,000	5,930			70
X71B3	173,700	183,500	1.6	50,000	7,550			
63B3	155,600	168,400	1.6	60,000	2,600			50
76A1	161,700	173,300	1.6	60,000	3,130			40
75B2	169,900	180,100	1.6	60,000	5,250			45
65B3	162,000	171,700	1.6	70,000	1,060	0.09	.12	60
85B2	160,200	171,800	1.6	70,000	2,240	0.06	.12	125
47A1	160,000	171,200	1.8	30,000	101,600			45
47A2	160,000	171,200	1.8	30,000	121,900			45
147A1	155,900	168,900	1.8	30,000	62,200			60

SPECIMEN DATA
Sheet 2 of 7

TABLE I

SPECIMEN NO.	STRENGTH (PSI) YIELD	STRENGTH (PSI) TENSILE	DIAMETER RATIO	TEST PRESSURE (PSI)	CYCLES TO FAILURE	FRACTURE AREA (in^2)	FRACTURE DEPTH (in)	AVG. SURFACE FINISH MICRO-IN
				NA - NON-AUTOFRETTAGED				
147A2	155,900	168,900	1.8	30,000	45,000			70
147A3	155,900	168,900	1.8	30,000	40,300	0.48	.36	
64A2	155,500	168,800	1.8	40,000	34,800			35
47B1	156,000	167,900	1.8	40,000	25,600	0.36	.34	60
47B2	156,000	167,900	1.8	40,000	27,600	0.34	.30	35
146A2	156,700	167,400	1.8	40,000	10,310			90
50A1	157,000	170,800	1.8	50,000	9,380			110
50A2	157,000	170,800	1.8	50,000	11,100			90
57B1	160,700	172,800	1.8	50,000	9,210			40
69B1	156,200	168,800	1.8	50,000	11,580			45
70B1	165,400	176,400	1.8	50,000	12,620	0.28		
113B2	160,700	166,200	1.8	50,000	6,060			45
50B1	166,400	177,100	1.8	60,000	8,620			70
50B2	166,400	177,100	1.8	60,000	5,850			80
50B3	166,400	177,100	1.8	60,000	7,440			40
57B3	160,700	172,800	1.8	60,000	7,680			40
66B1	151,800	166,700	1.8	60,000	6,030			75
62B1	156,100	167,700	1.8	60,000	9,700	0.17		
70B2	165,400	176,400	1.8	60,000	8,800			65
30B2	169,500	178,800	1.8	70,000	3,950			
57A1	157,700	169,000	1.8	70,000	6,280	0.15		
76B1	157,200	168,800	1.8	70,000	3,580	0.16	.24	55
143A1	161,300	172,000	2.0	40,000	34,500	0.55	.41	50
143A2	161,300	172,000	2.0	40,000	43,600	0.60	.41	45
147B1	155,100	167,500	2.0	40,000	35,600	0.60	.37	40
43A2	158,200	169,700	2.0	40,000	55,900	0.49	.37	35
43B1	160,600	171,200	2.0	50,000	8,780			35
43B2	160,600	171,200	2.0	50,000	12,240	0.44	.36	30

SPECIMEN DATA
Sheet 3 of 7

TABLE I

SPECIMEN NO.	STRENGTH (PSI) YIELD	STRENGTH (PSI) TENSILE	DIAMETER RATIO	TEST PRESSURE (PSI)	CYCLES TO FAILURE	FRACTURE AREA (in^2)	FRACTURE DEPTH (in)	AVG. SURFACE FINISH MICRO-IN
				NA - NON-AUTOFRETTAGED				
147B2	155,100	167,500	2.0	50,000	13,670	0.46	.36	70
143A3	161,300	172,000	2.0	50,000	11,780			75
43A3	158,200	169,700	2.0	60,000	8,850			55
43B3	160,600	171,200	2.0	60,000	6,500	0.24	.33	40
65A2	161,600	172,100	2.0	60,000	7,860			
65A3	161,600	172,100	2.0	60,000	7,640	0.24	.30	40
57A3	157,700	169,000	2.0	60,000	7,810	0.24	.30	16
65A1	161,600	172,100	2.0	70,000	5,670	0.30	.25	95
143B1	155,900	166,900	2.0	70,000	6,920			35
143B2	155,900	166,900	2.0	70,000	6,420			65
143B3	155,900	166,900	2.0	70,000	7,820			60
24B3	168,800	177,100	2.0	70,000	7,510	0.29	.25	40
				A - AUTOFRETTAGED				
82B2	160,900	171,200	1.4	29,000	44,400			
54A1	161,600	171,900	1.4	29,000	49,400			
86B2	160,900	172,800	1.4	30,000	32,700	0.09	.15	115
87A(1)	150,200	163,600	1.4	30,000	49,700			85
65B2	162,000	171,700	1.4	40,000	6,370	0.06		
76B2	157,200	168,800	1.4	40,000	5,270	0.05		
X66A2	180,800	188,700	1.4	40,000	7,380			
X66A3	180,800	188,700	1.4	40,000	7,220			
38A2T	165,600	177,000	1.4	50,000	2,590	0.06		
38A3T	165,600	177,000	1.4	50,000	2,500			40
38B3T	168,600	172,500	1.4	50,000	2,290			30
63B2	155,600	168,400	1.4	50,000	2,930			30
87A3	150,100	163,900	1.4	50,000	1,740	0.04		
113B3	160,700	166,200	1.4	50,000	3,380	0.04	.09	55

SPECIMEN DATA
Sheet 4 of 7

TABLE I

SPECIMEN NO.	STRENGTH (PSI) YIELD	STRENGTH (PSI) TENSILE	DIAMETER RATIO	TEST PRESSURE (PSI)	CYCLES TO FAILURE	FRACTURE AREA (in^2)	FRACTURE DEPTH (in)	AVG. SURFACE FINISH MICRO-IN
				A - AUTOFRETTAGED				
83A3	153,700	165,900	1.6	40,000	38,860			25
83B1	159,600	169,700	1.6	40,000	17,860	0.25	.24	70
90A1	163,000	173,400	1.6	40,000	70,000			
69A2	163,200	173,600	1.6	40,000	70,000			
82B1	160,800	171,200	1.6	40,000	70,000			
79B1	155,900	166,200	1.6	40,000	36,800			60
77B2T	158,600	170,600	1.6	50,000	10,140	0.11		
77B3T	158,600	170,600	1.6	50,000	8,090			
67B2T	158,500	170,300	1.6	50,000	7,620	0.14		
67B3T	158,500	170,300	1.6	50,000	6,180			30
87A3T	150,100	163,900	1.6	50,000	13,540			55
85B1	160,200	171,800	1.6	50,000	11,630			100
68A1	161,500	173,200	1.6	50,000	13,670			80
66A1	155,400	166,600	1.6	50,000	7,110			90
86A2	159,800	170,700	1.6	50,000	7,910			45
88A3	160,300	170,600	1.6	50,000	5,990			80
73A2T	158,500	170,000	1.6	60,000	5,220			50
73B2T	158,500	170,000	1.6	60,000	6,030			35
70A3	150,500	167,200	1.6	60,000	4,910	0.09	.15	30
67A2	157,000	169,000	1.6	60,000	2,590			35
67A3	157,000	169,000	1.6	60,000	2,960			35
68A2	161,500	173,200	1.6	60,000	5,410	0.11		
68A3	161,500	173,200	1.6	60,000	5,910			80
66B2T	151,800	166,700	1.6	60,000	4,380			50
66B3T	151,800	166,700	1.6	60,000	2,680			55
79A2	153,100	167,900	1.6	60,000	2,440			80
87A2	150,100	163,900	1.6	60,000	5,580			55
87B2	156,600	168,000	1.6	60,000	4,170			80
92B1	151,400	164,500	1.6	60,000	6,310			50

SPECIMEN DATA
Sheet 5 of 7

TABLE I

SPECIMEN NO.	STRENGTH (PSI) YIELD	STRENGTH (PSI) TENSILE	DIAMETER RATIO	TEST PRESSURE (PSI)	CYCLES TO FAILURE	FRACTURE AREA (in^2)	FRACTURE DEPTH (in)	AVG. SURFACE FINISH MICRO-IN
				A - AUTOFRETTAGED				
76A3	161,700	173,300	1.6	70,000	2,020			
73A1	158,500	170,000	1.6	70,000	2,600	0.07	.14	50
73A3	158,500	170,000	1.6	70,000	2,730			55
65B1	162,000	171,700	1.6	70,000	1,600			20
X98A3	178,000	188,000	1.8	47,000	77,170			
X98A2	178,000	188,000	1.8	47,000	80,150			
X101A3	173,000	183,000	1.8	47,000	169,500			
79A3T	153,100	167,900	1.8	60,000	8,840			100
92B3T	151,400	164,500	1.8	60,000	11,000			50
75B3T	169,900	180,100	1.8	60,000	15,320			40
87A1	150,100	163,900	1.8	60,000	9,150			50
82A1	163,100	174,000	1.8	60,000	18,280			60
67B1	158,500	170,300	1.8	70,000	2,880	0.18	.24	65
79A1	153,100	167,900	1.8	70,000	4,170			80
79B3	155,900	166,200	1.8	70,000	7,670			60
90A3T	163,000	173,400	1.8	70,000	8,400			50
56B3T	174,400	183,000	1.8	70,000	13,700			
83B2	168,000	178,400	1.8	70,000	12,200			
71A1	165,500	175,200	1.8	80,000	4,620			110
56A3T	160,000	170,800	1.8	80,000	3,150			50
X56A3	170,000	181,100	1.8	80,000	6,530			
54B2T	173,700	182,000	1.8	80,000	7,370			
69A1	163,200	173,600	1.8	90,000	2,810			
56A1T	160,000	170,800	1.8	90,000	2,660			
56B1	174,400	183,000	1.8	90,000	4,140			
56B2T	174,400	183,000	1.8	90,000	3,860	0.11	.15	55
71B1	162,400	172,400	1.8	100,000	940			
89B1T	162,800	173,300	1.8	100,000	1,850	0.09	.13	50

SPECIMEN DATA
Sheet 6 of 7

TABLE I

SPECIMEN NO.	STRENGTH (PSI) YIELD	STRENGTH (PSI) TENSILE	DIAMETER RATIO	TEST PRESSURE (PSI)	CYCLES TO FAILURE	FRACTURE AREA (in^2)	FRACTURE DEPTH (in)	AVG. SURFACE FINISH MICRO-IN
				A - AUTOFRETTAGED				
90A2	163,000	173,400	1.8	100,000	1,860			
78B1T	164,400	173,300	1.8	100,000	1,220			
X82A2	168,300	182,000	2.0	61,000	41,800			
X44B2	171,600	184,300	2.0	61,000	45,900			
X88B3	172,000	182,000	2.0	61,000	53,700			
X85B3	168,400	179,700	2.0	70,000	12,790			60
82A3	163,100	173,900	2.0	70,000	16,460			
X41B1	168,400	179,700	2.0	70,000	11,800			
X53A1	164,900	175,100	2.0	90,000	4,100			
X88B1	168,400	179,700	2.0	90,000	4,120			
X39B2	172,400	180,600	2.0	100,000	1,780			
X53A3	164,900	175,100	2.0	100,000	2,430			
X85B2	168,400	179,700	2.0	100,000	2,170			
X39B3	172,400	180,600	2.0	100,000	2,000			

SPECIMEN DATA
Sheet 7 of 7

TABLE I

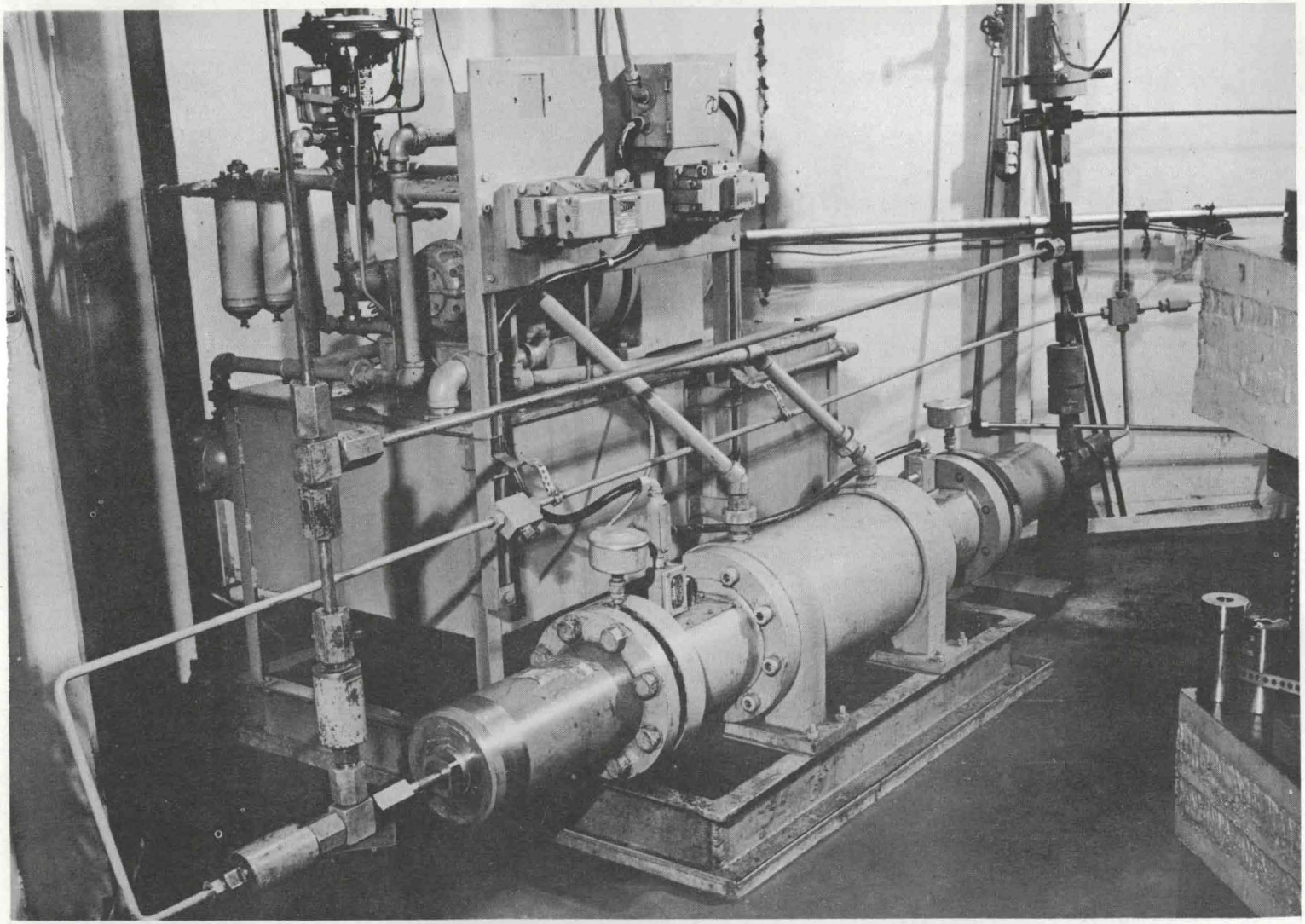

FIGURE 1. PRESSURE SOURCE FOR 80,000 POUNDS PER SQUARE INCH FATIGUE SYSTEM

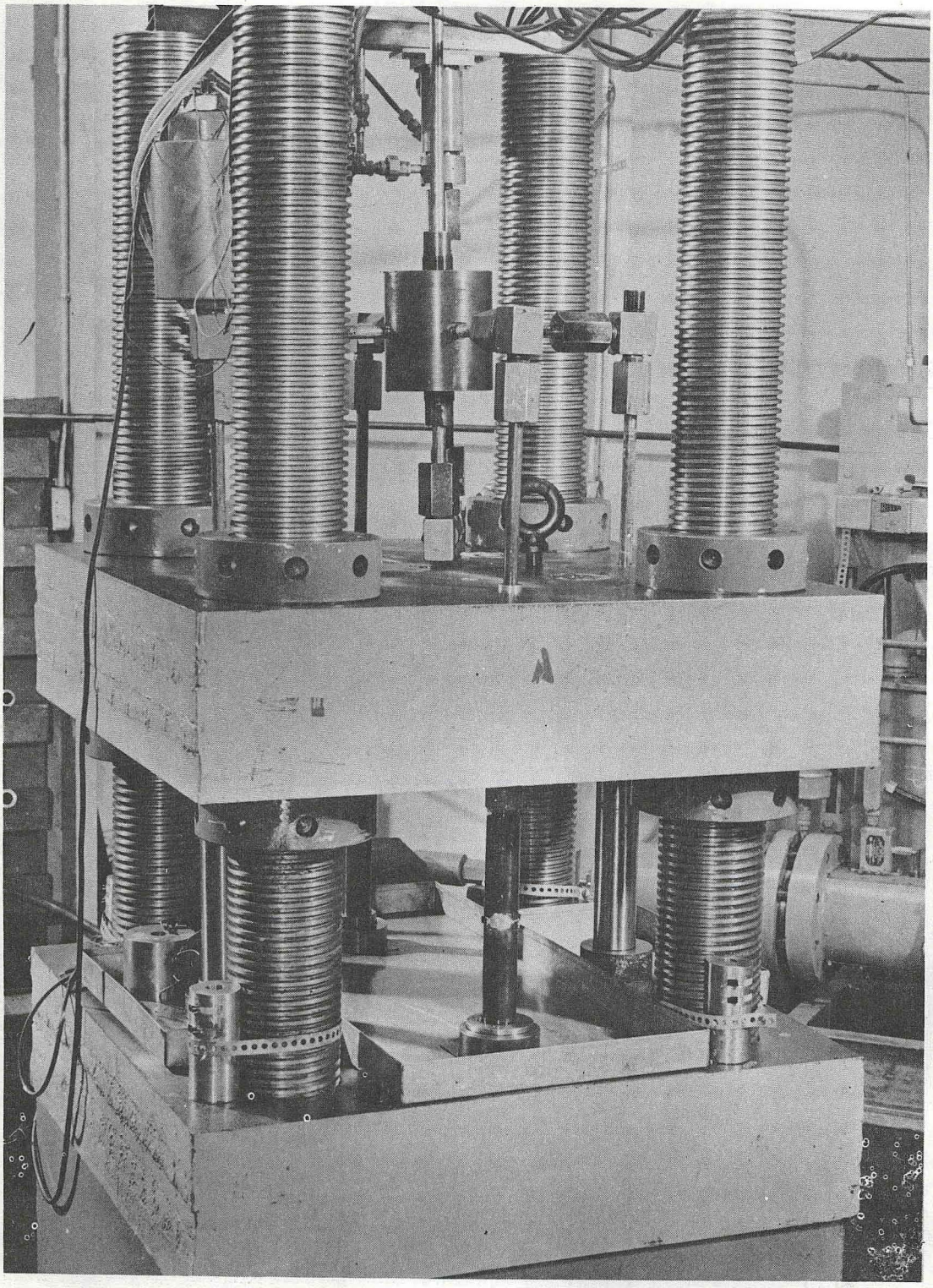

FIGURE 2. HOLDING PRESS AND SPECIMENS FOR 80,000 PER SQUARE INCH FATIGUE SYSTEM

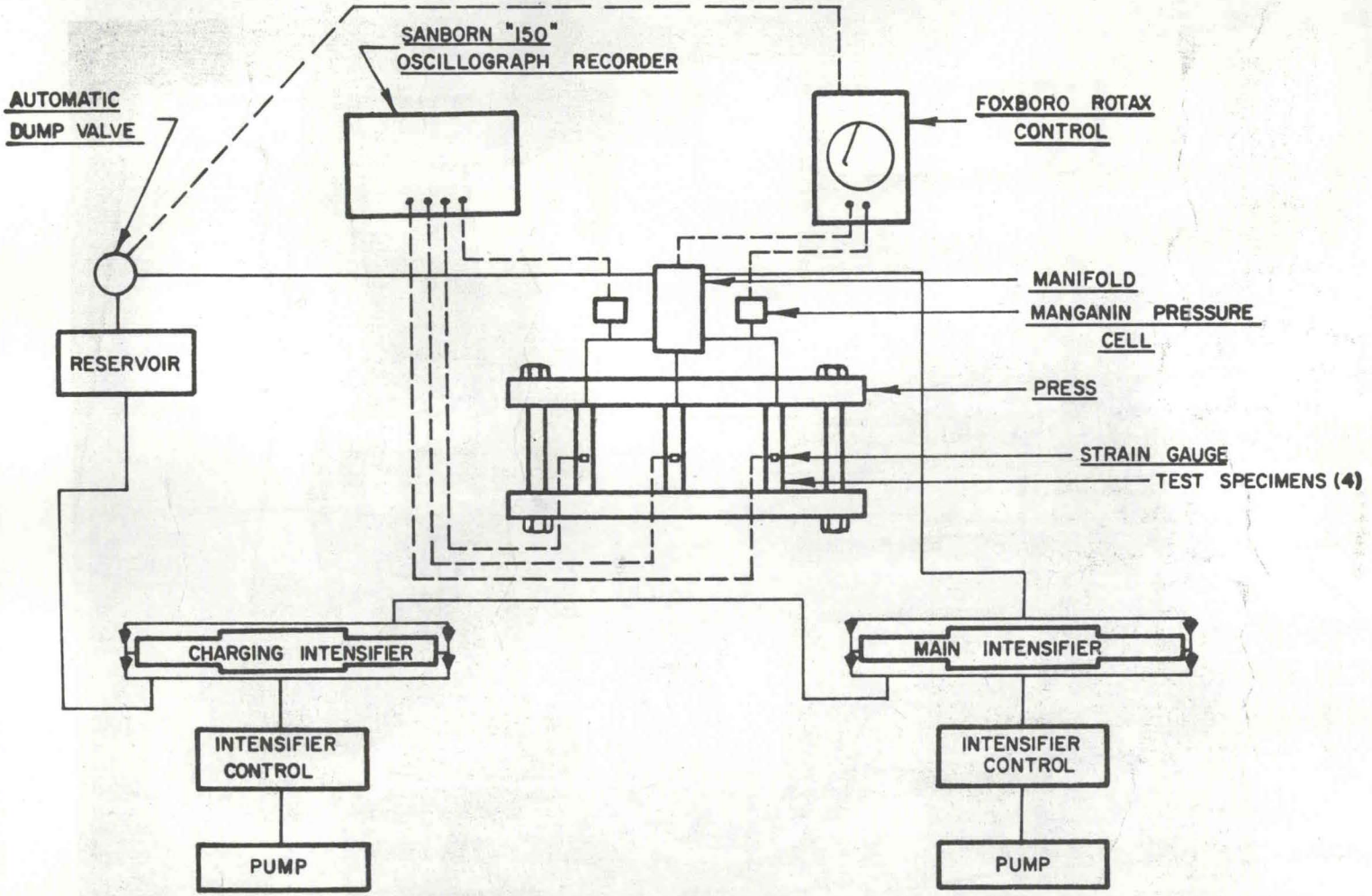

FIGURE 3. SCHEMATIC OF 80,000 PSI FATIGUE SYSTEM

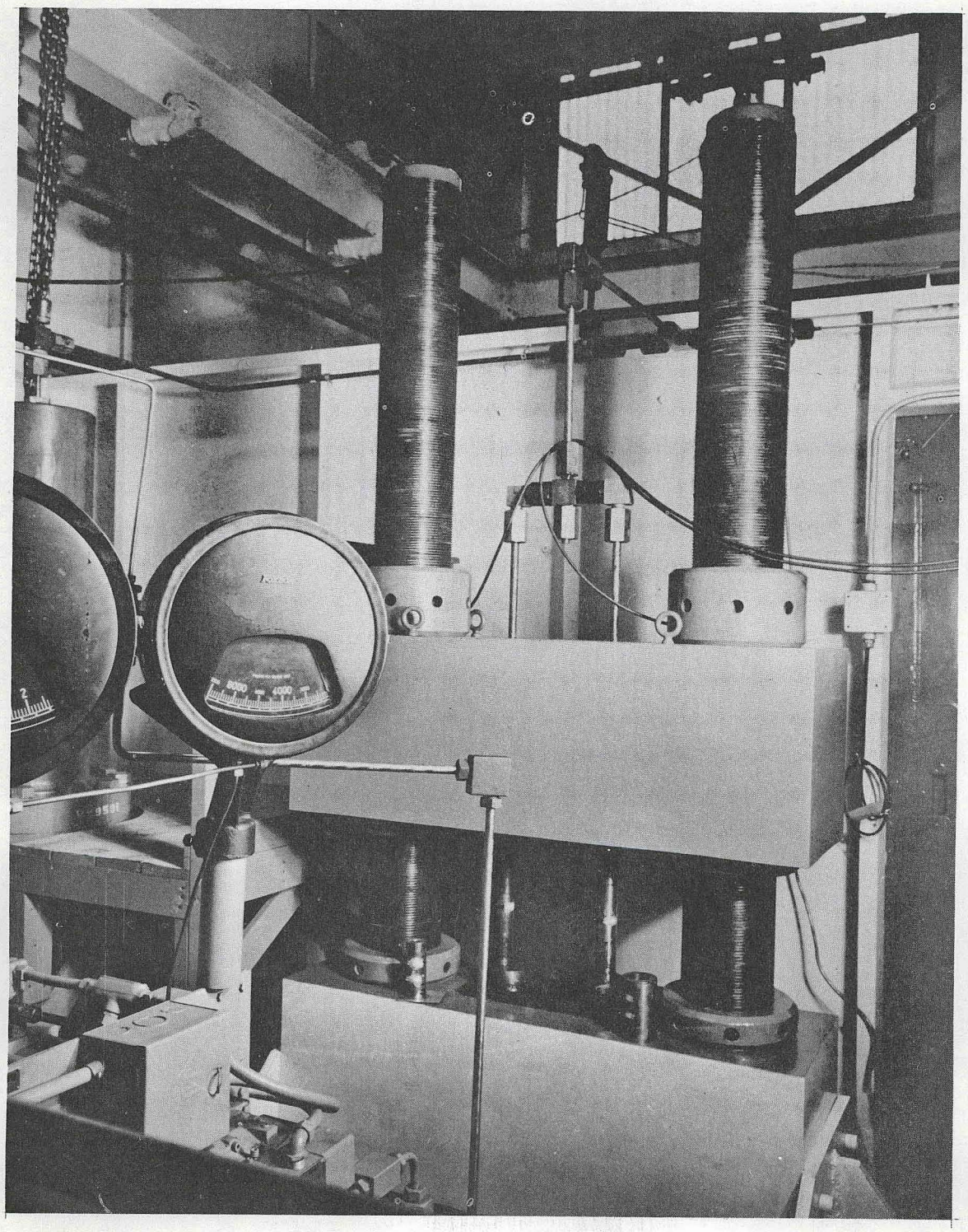

FIGURE 4. 150,000 POUNDS PER SQUARE INCH FATIGUE SYSTEM

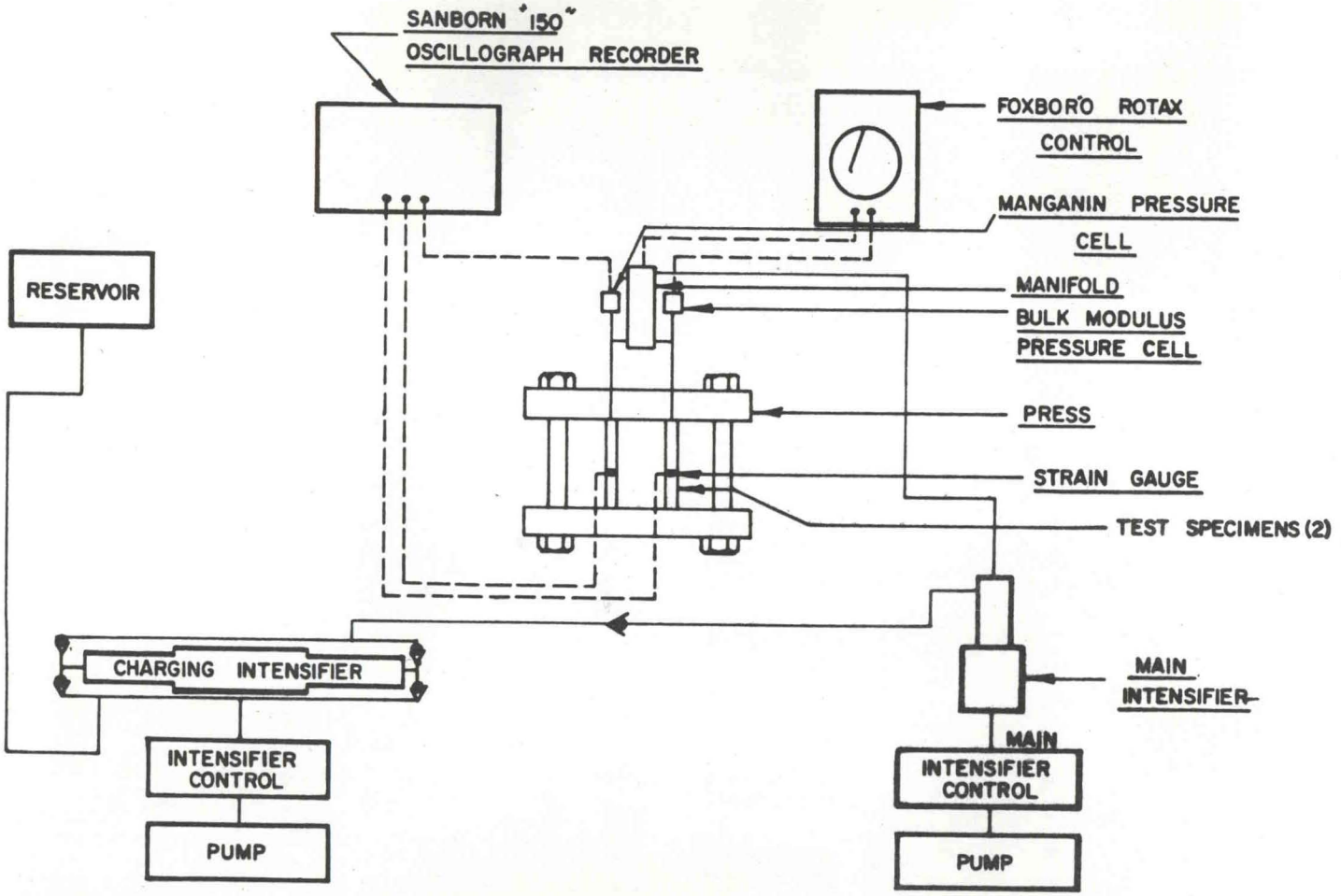

FIGURE 5. SCHEMATIC OF 150,000 PSI FATIGUE SYSTEM

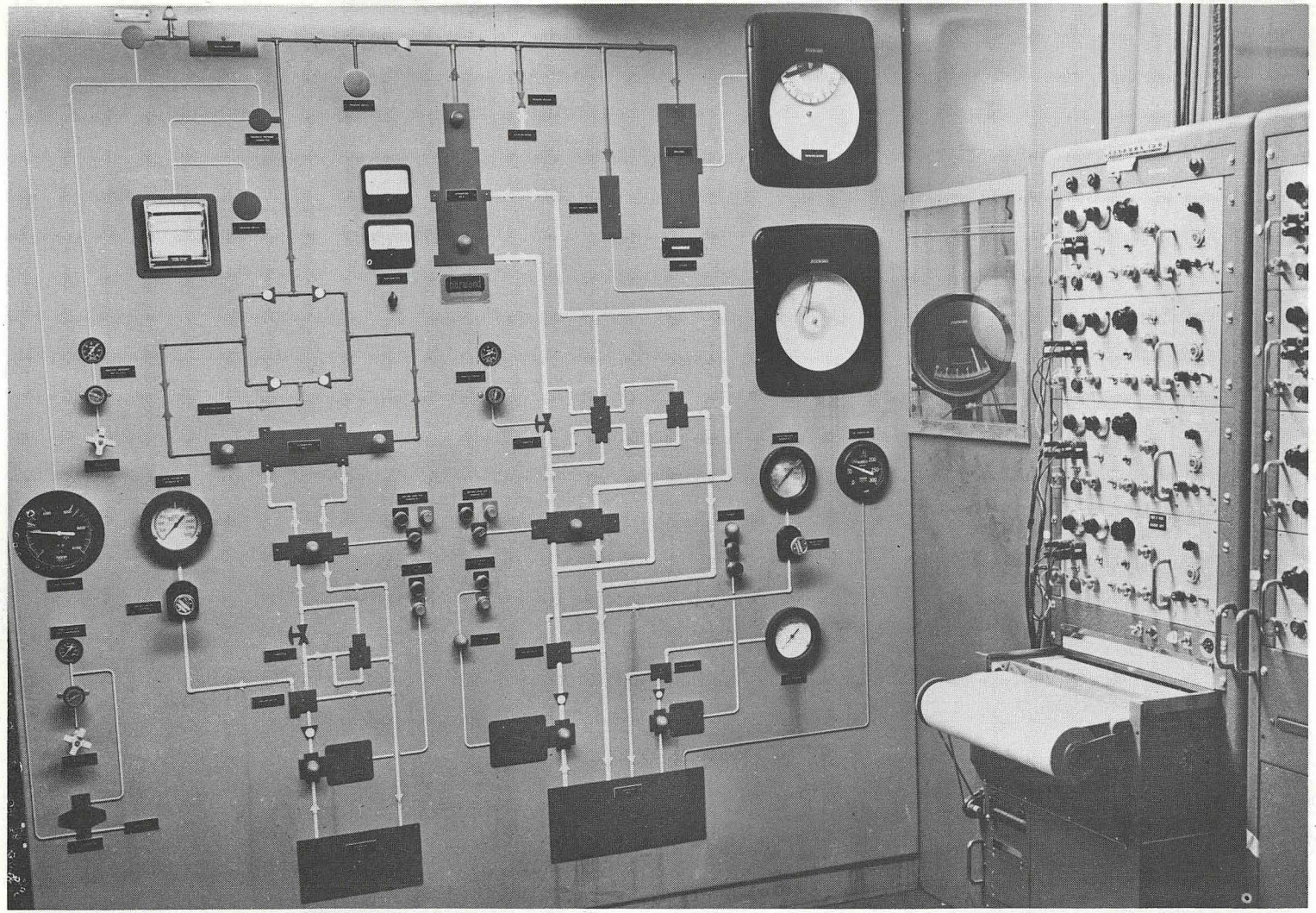

FIGURE 6. CONTROLS AND INSTRUMENTATION FOR 150,000 POUNDS PER SQUARE INCH FATIGUE SYSTEM

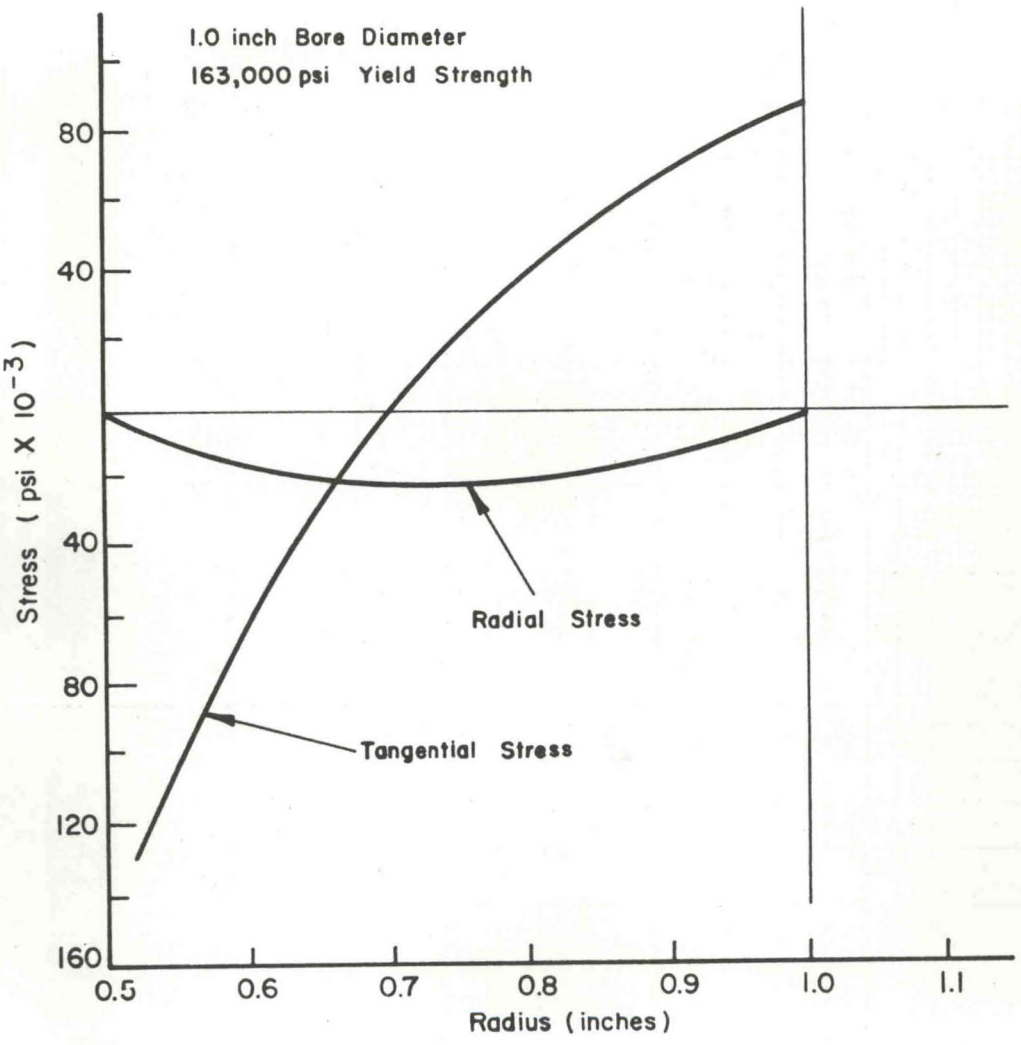

FIGURE 7. RESIDUAL STRESS DISTRIBUTION FOR A 2.0 DIAMETER RATIO 100 PERCENT OVERSTRAINED CYLINDER

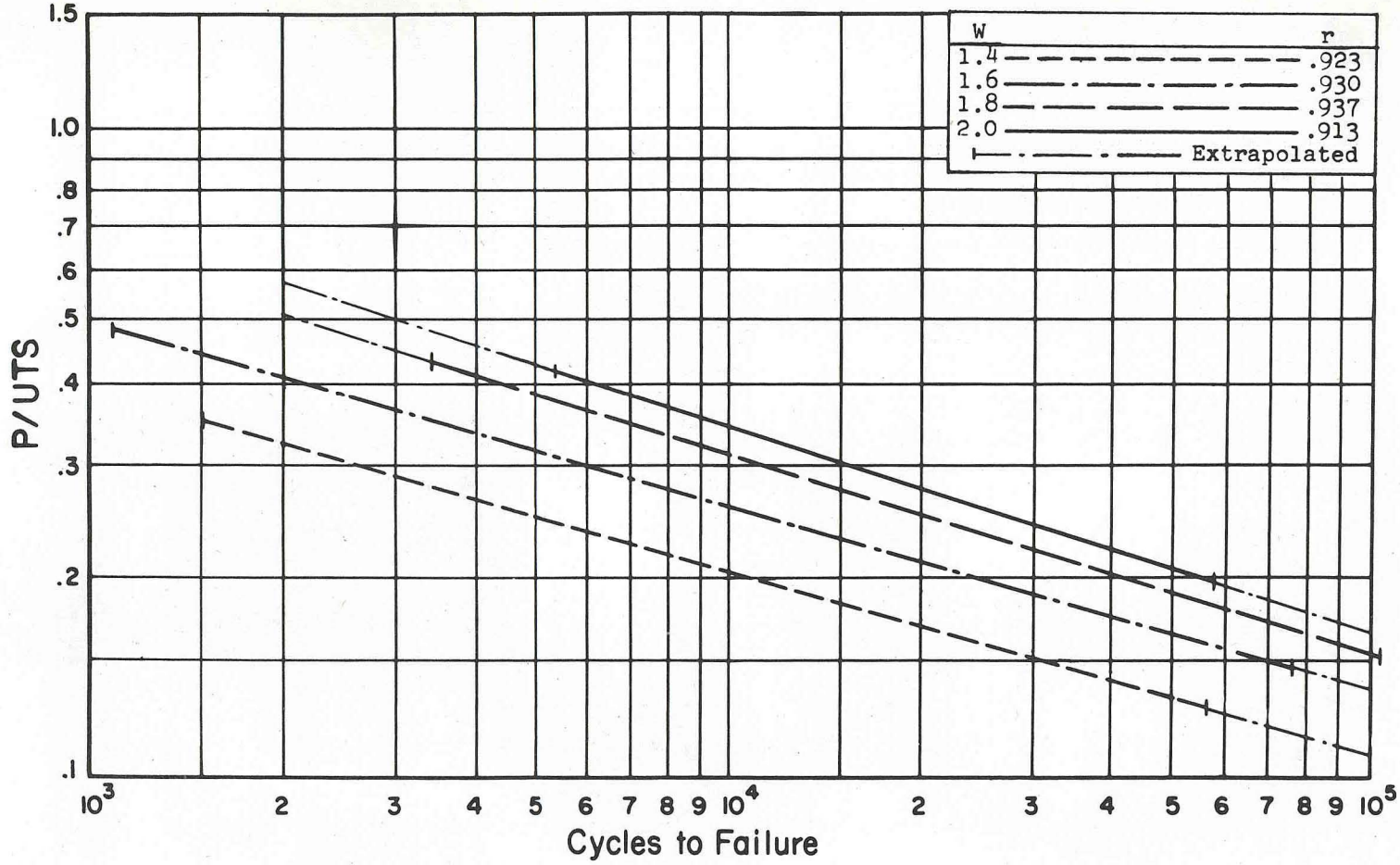

FIGURE 8. PRESSURE vs CYCLES TO FAILURE

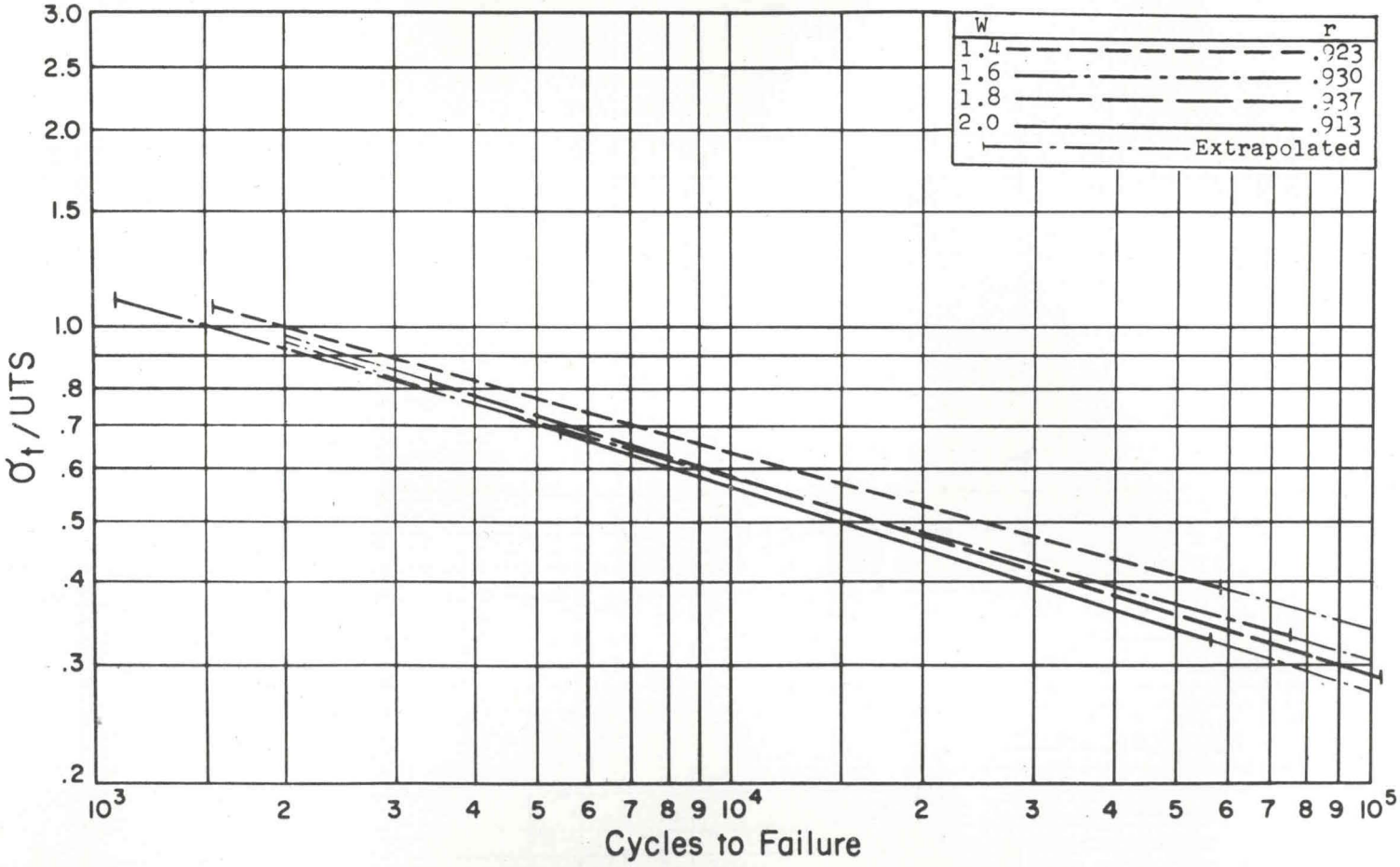

FIGURE 9. TANGENTIAL BORE STRESS vs CYCLES TO FAILURE

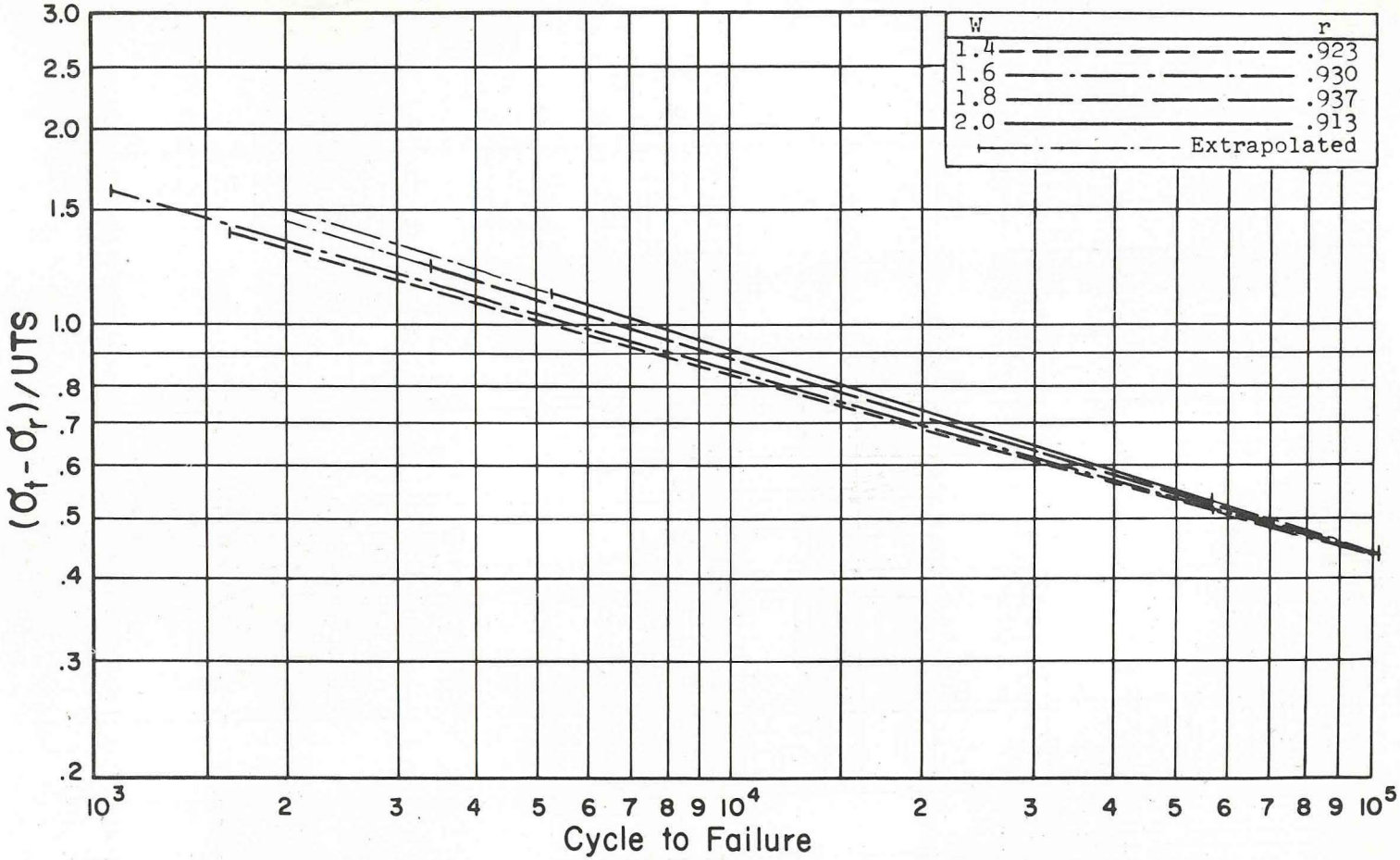

FIGURE 10. DIFFERENCE IN PRINCIPAL BORE STRESS vs CYCLES TO FAILURE

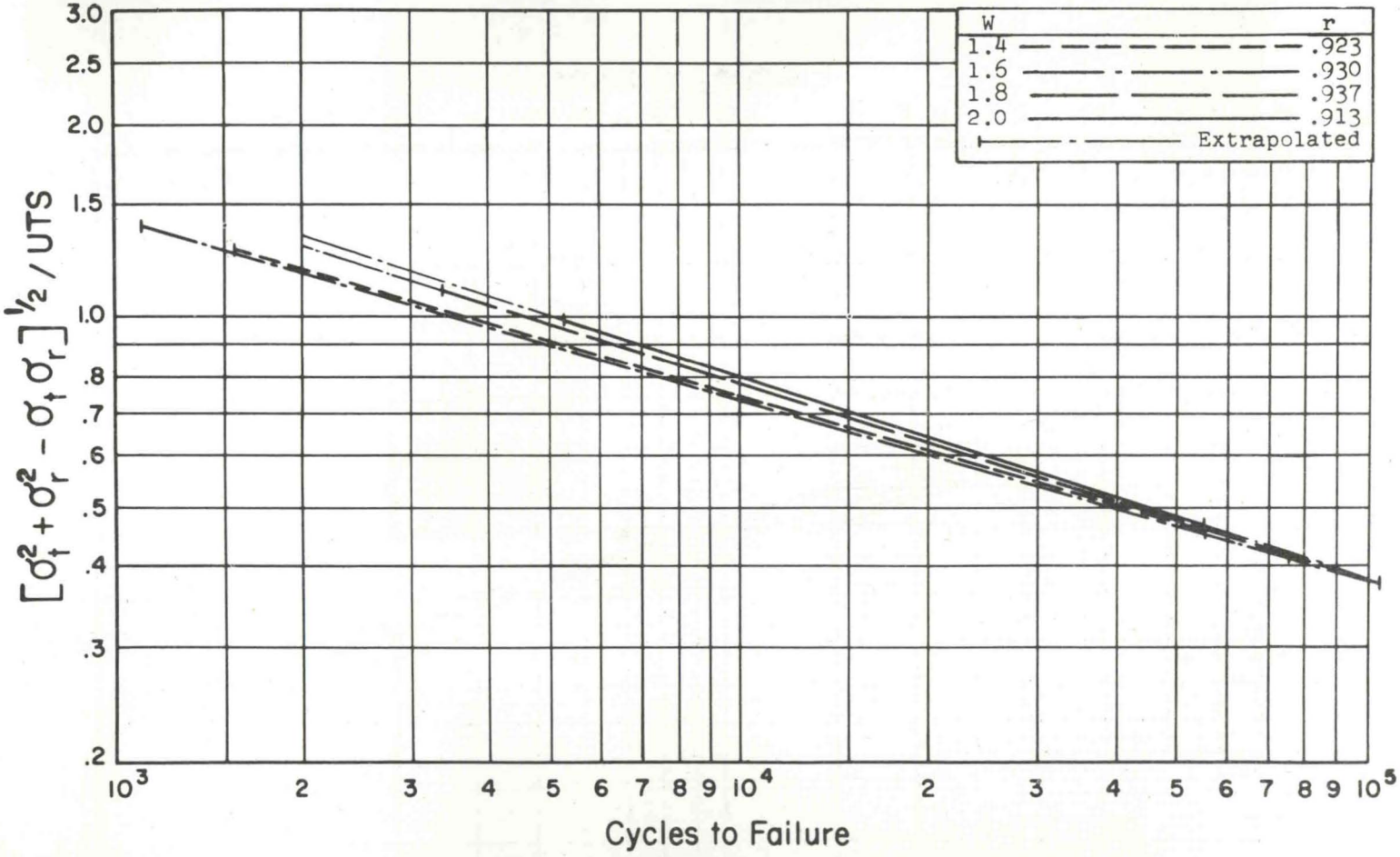

FIGURE 11. OCTAHEDRAL STRESS PARAMETER vs CYCLES TO FAILURE

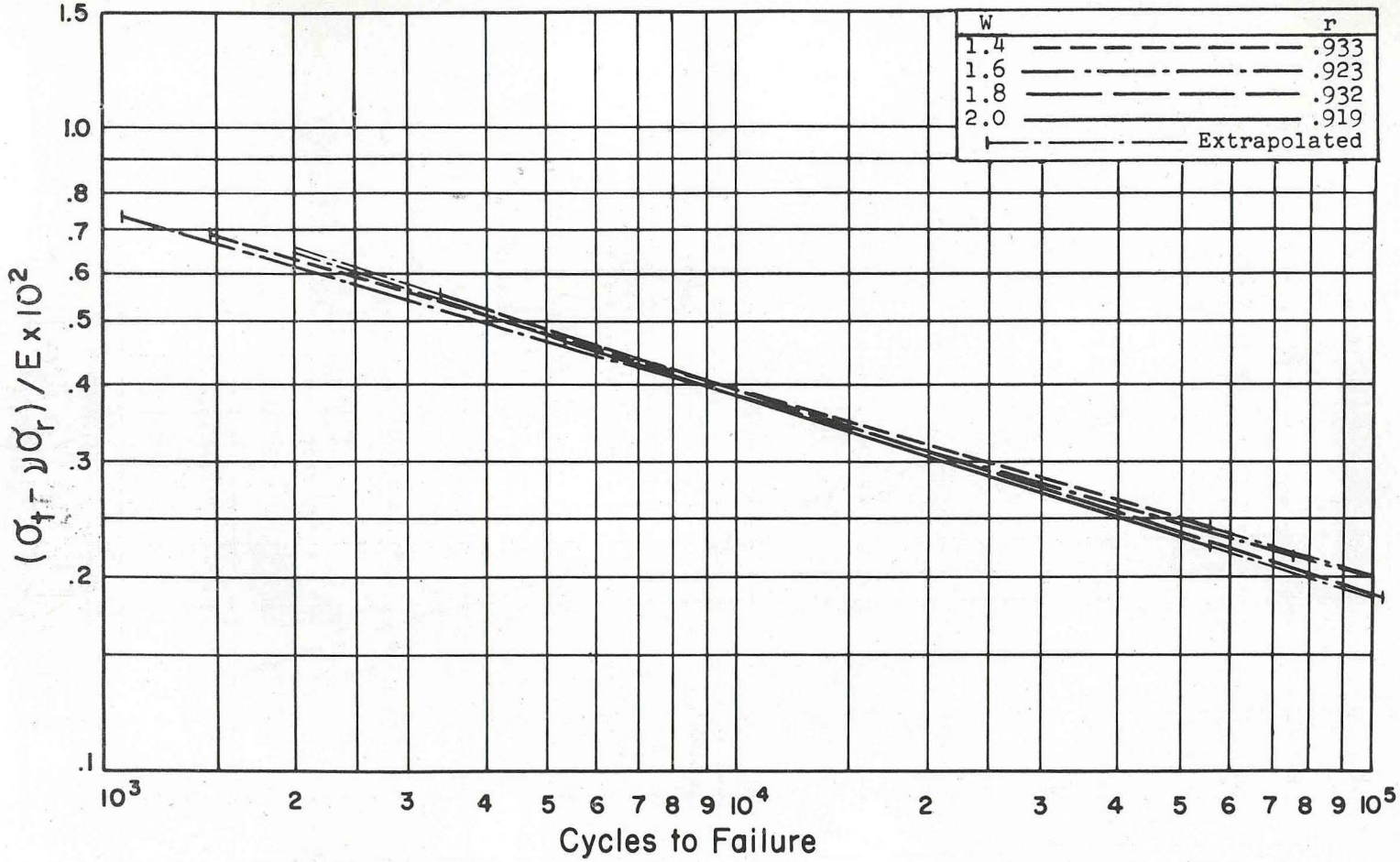

FIGURE 12. STRAIN PARAMETER vs CYCLES TO FAILURE

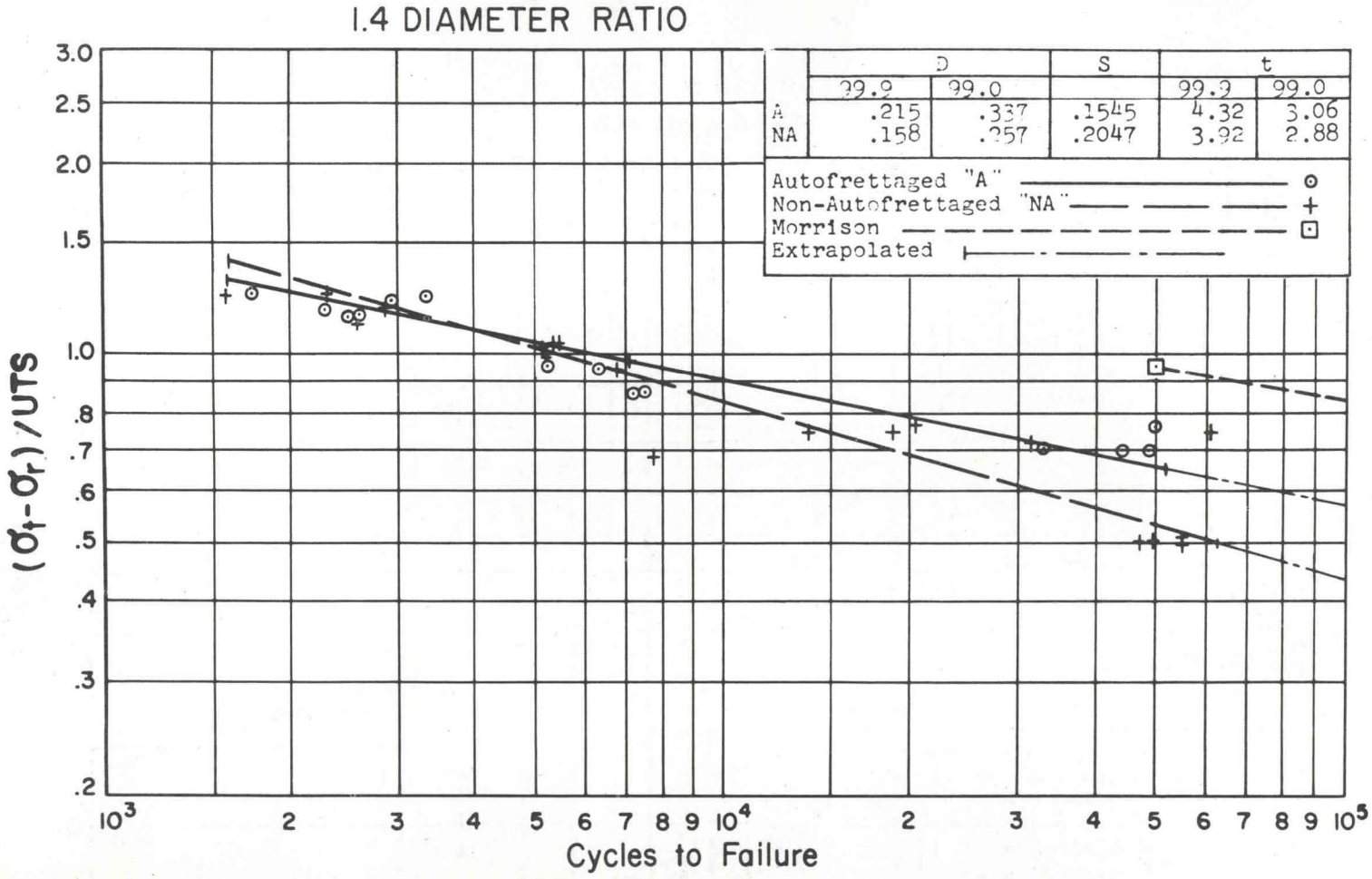

FIGURE 13. DIFFERENCE IN PRINCIPAL BORE STRESS vs CYCLES TO FAILURE FOR 1.4 DIAMETER RATIO

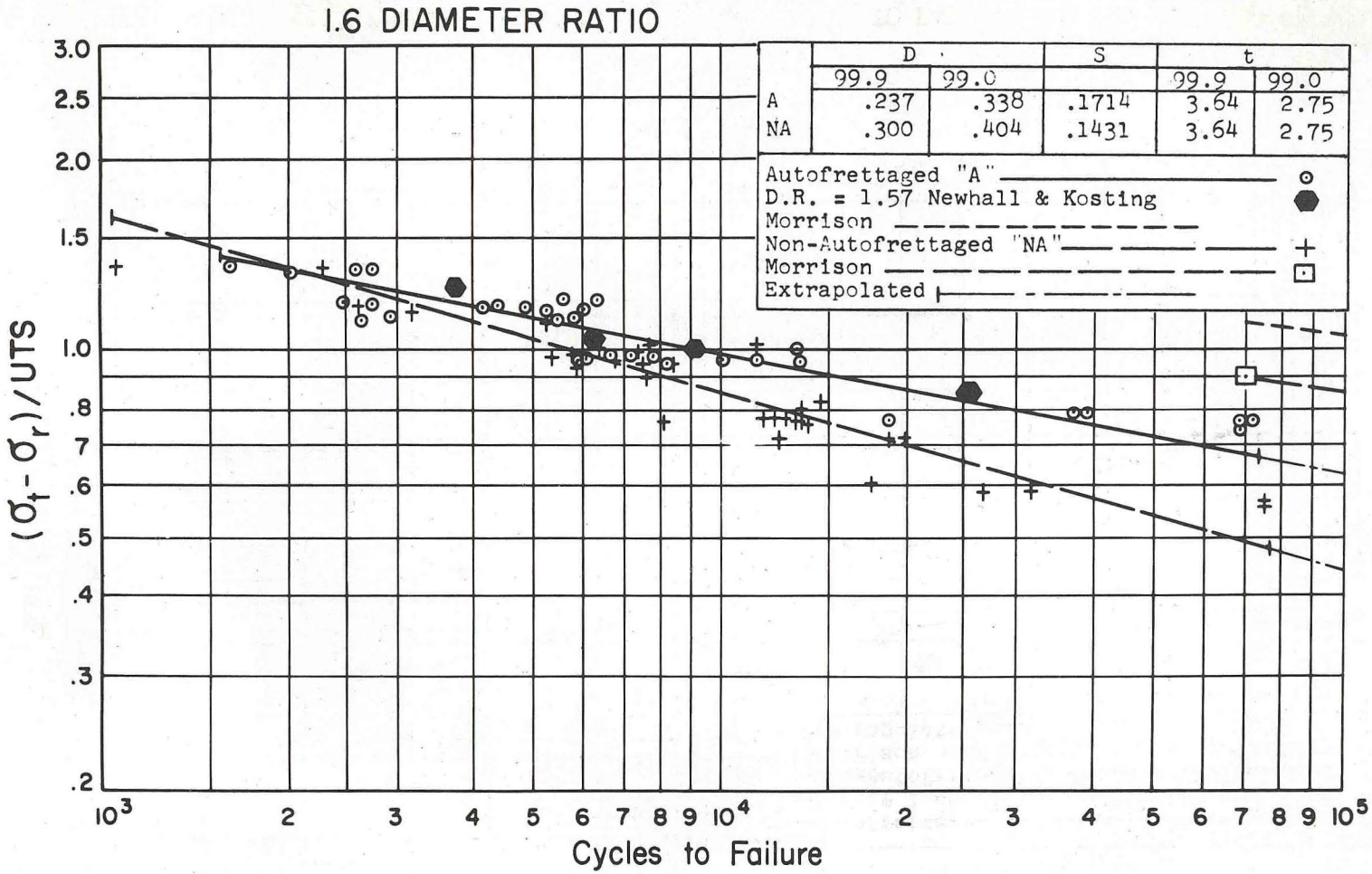

FIGURE 14. DIFFERENCE IN PRINCIPAL BORE STRESS vs CYCLES TO FAILURE FOR 1.6 DIAMETER RATIO

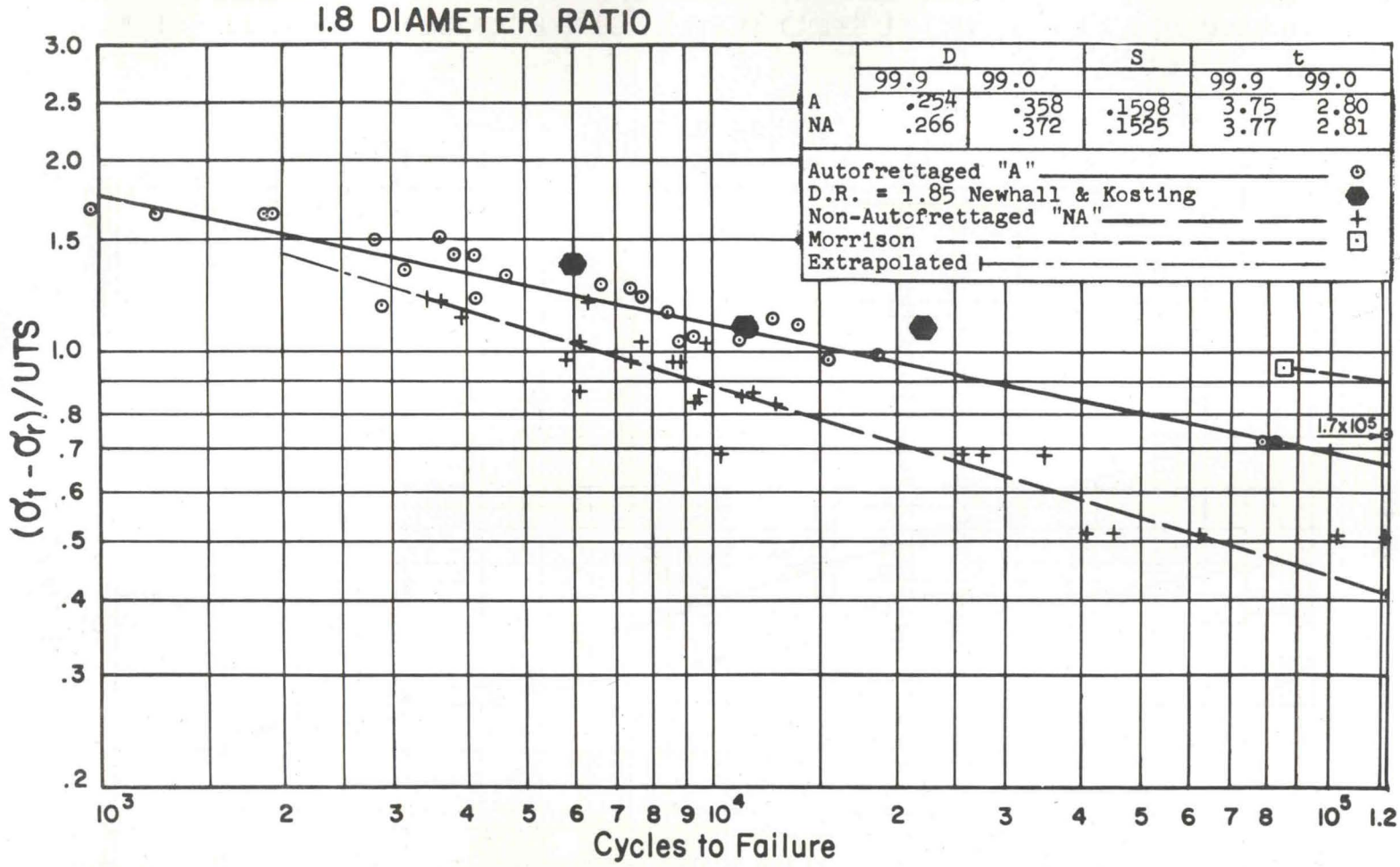

FIGURE 15. DIFFERENCE IN PRINCIPAL BORE STRESS vs CYCLES TO FAILURE FOR 1.8 DIAMETER RATIO

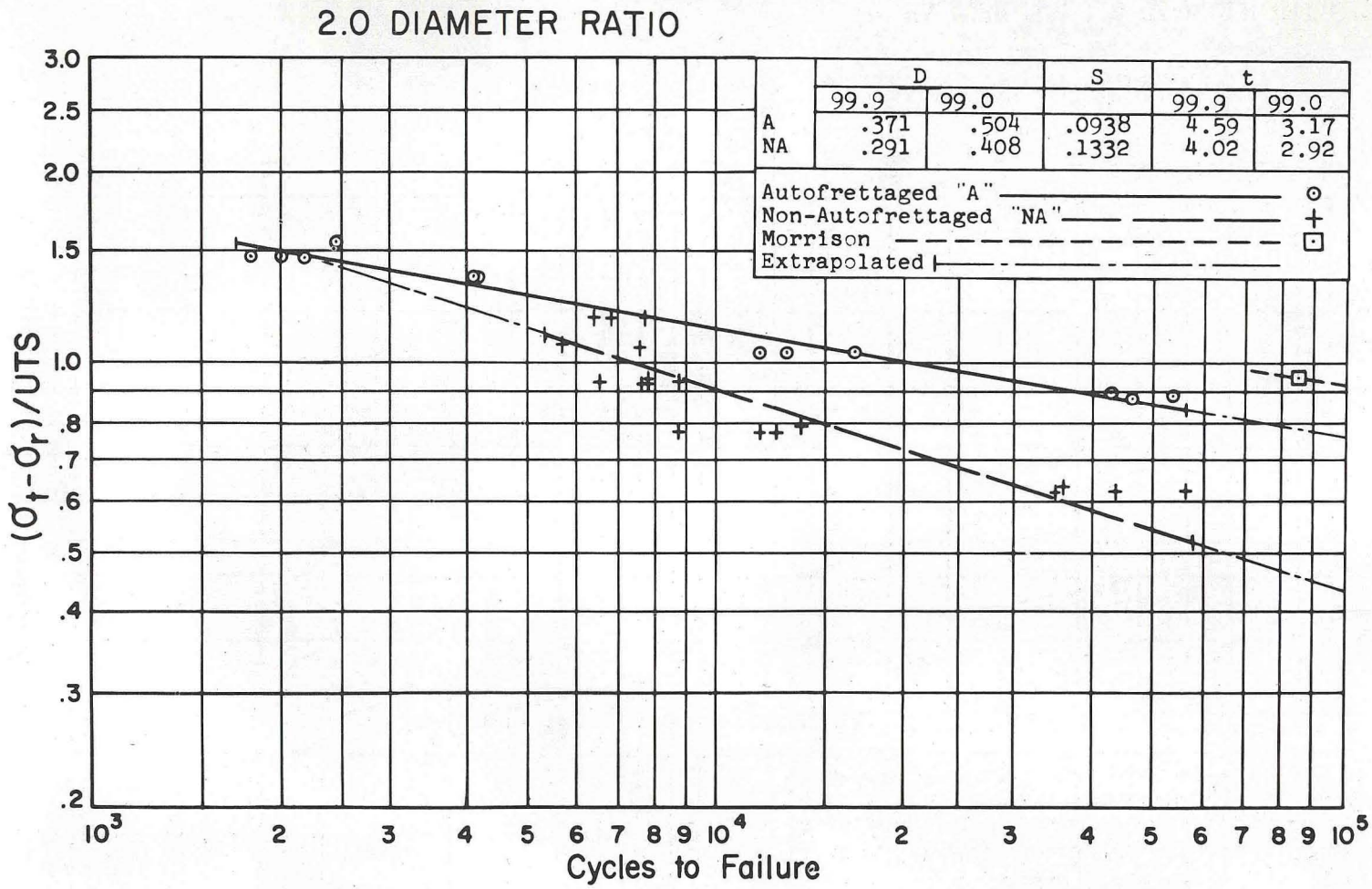

FIGURE 16. DIFFERENCE IN PRINCIPAL BORE STRESS vs CYCLES TO FAILURE FOR 2.0 DIAMETER RATIO

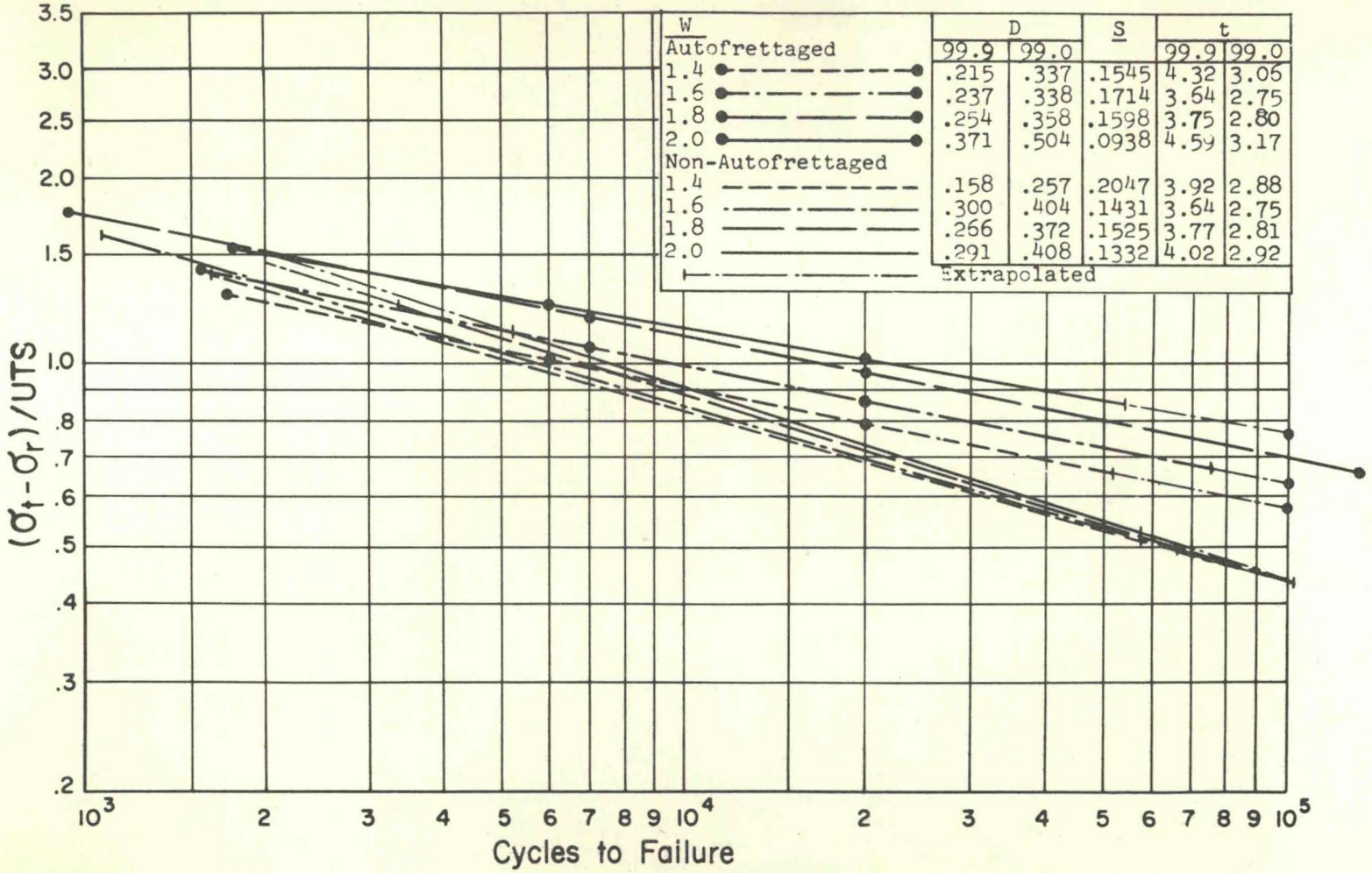

FIGURE 17. DIFFERENCE IN PRINCIPAL BORE STRESS vs CYCLES TO FAILURE FOR 1.4 - 2.0 DIAMETER RATIO

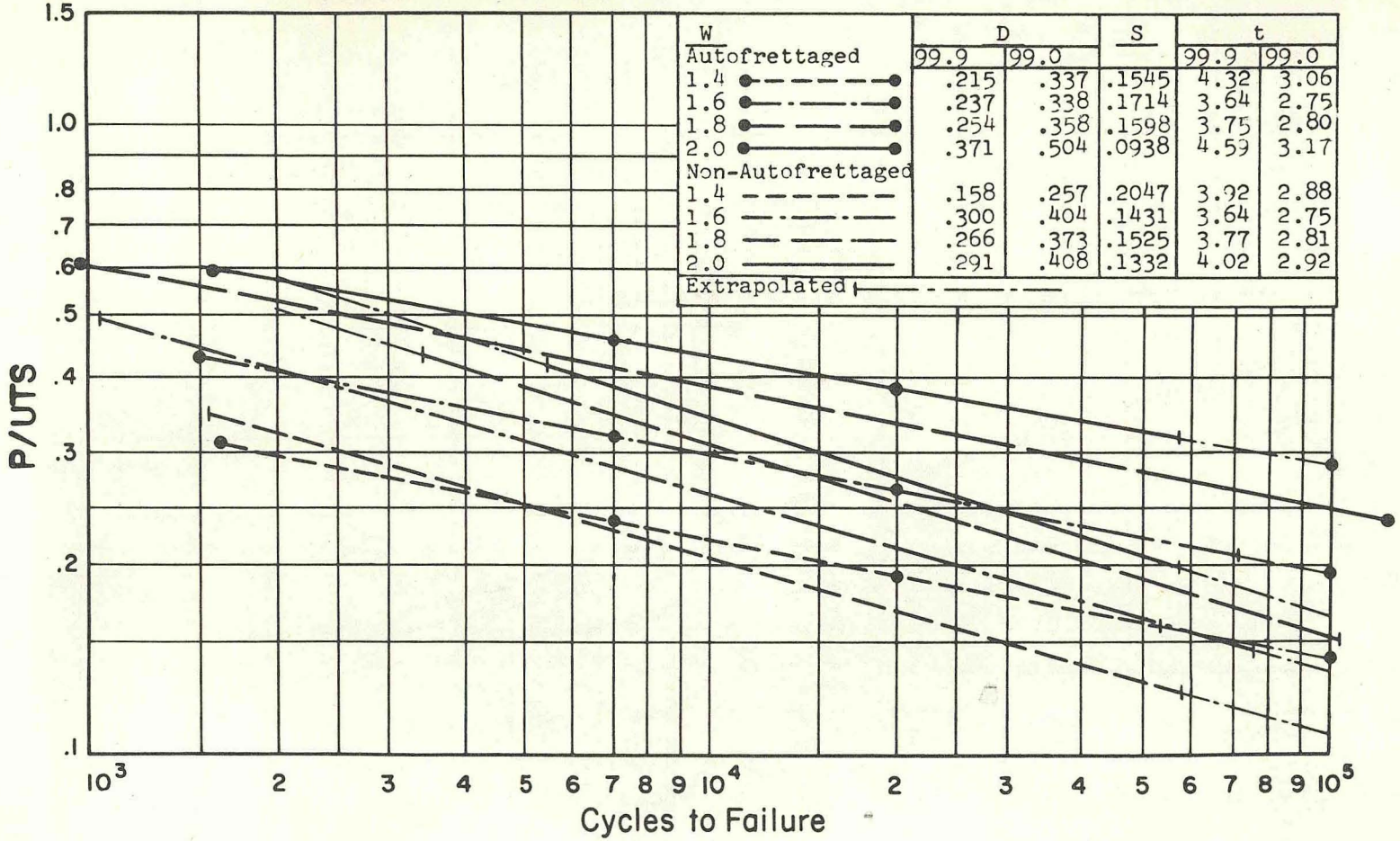

FIGURE 18. PRESSURE vs CYCLES TO FAILURE FOR 1.4 - 2.0 DIAMETER RATIO

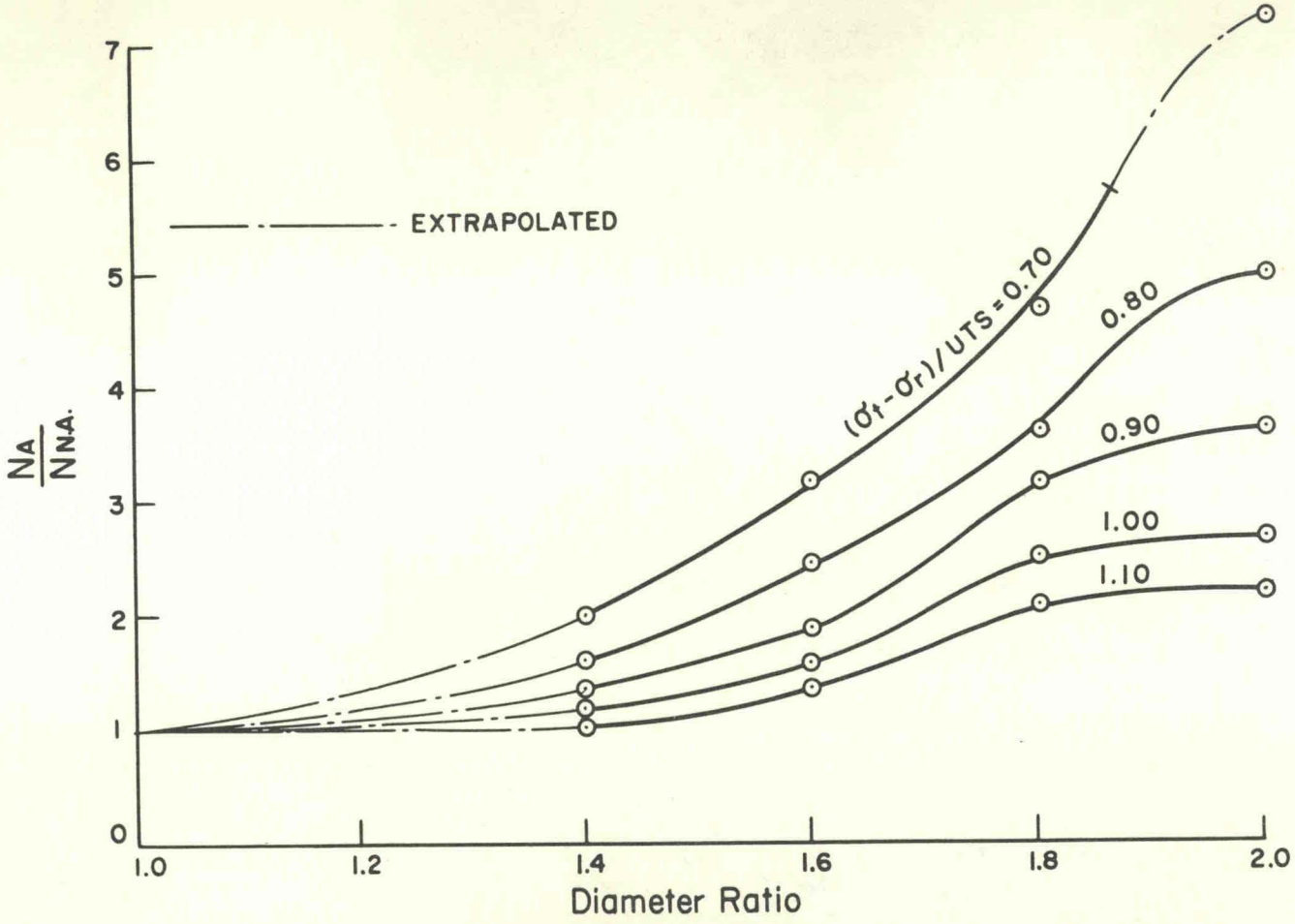

FIGURE 19. RATIO OF AUTOFRETTAGED TO NON-AUTOFRETTAGED CYCLES TO FAILURE vs DIAMETER RATIO

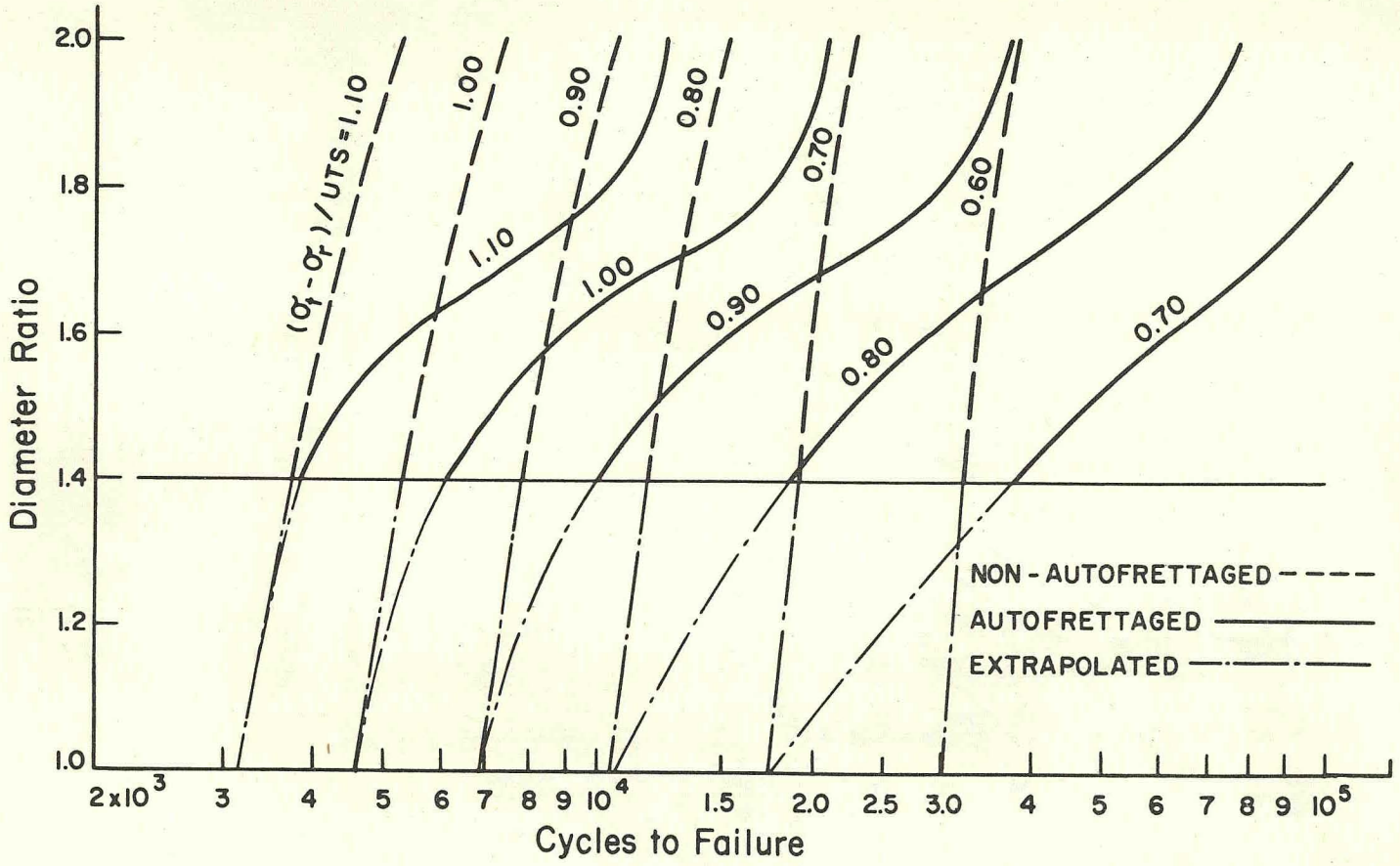

FIGURE 20. DIAMETER RATIO vs CYCLES TO FAILURE AT VARIOUS DIFFERENCES IN PRINCIPAL STRESS LEVEL

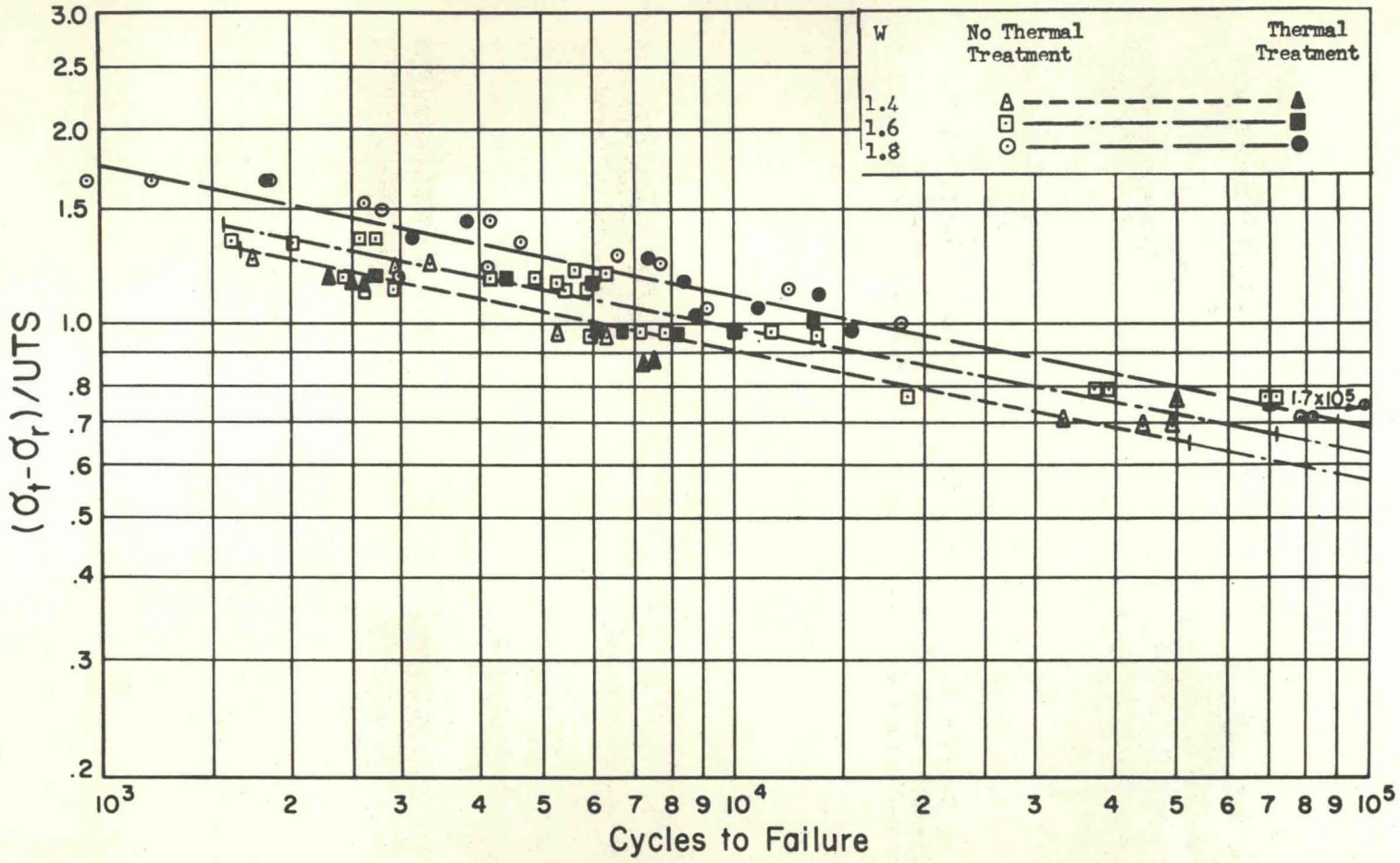

FIGURE 21. DIFFERENCE IN PRINCIPAL BORE STRESS vs CYCLES TO FAILURE SHOWING EFFECT OF THERMAL TREATMENT

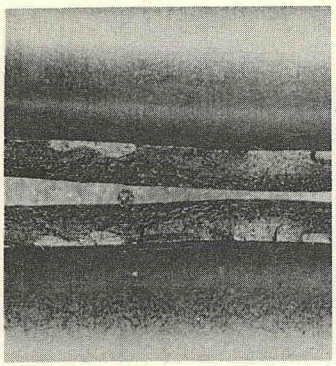

Diameter Ratio = 1.4
Test Pressure = 50,000 PSI
Cycles to Failure = 3,380

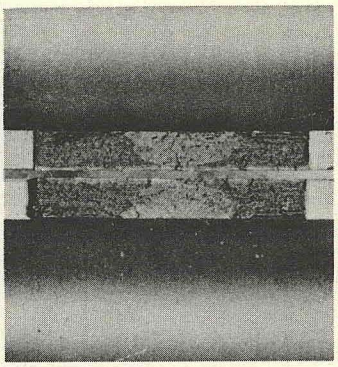

Diameter Ratio = 1.4
Test Pressure = 30,000 PSI
Cycles to Failure = 31,300

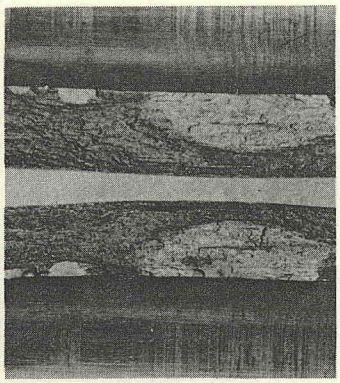

Diameter Ratio = 1.8
Test Pressure = 70,000 PSI
Cycles to Failure = 2,880

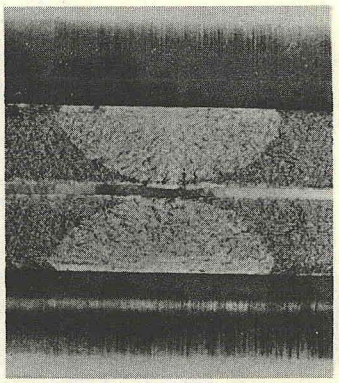

Diameter Ratio = 1.8
Test Pressure = 30,000 PSI
Cycles to Failure = 40,300

FIGURE 22. TYPICAL FATIGUE FRACTURES

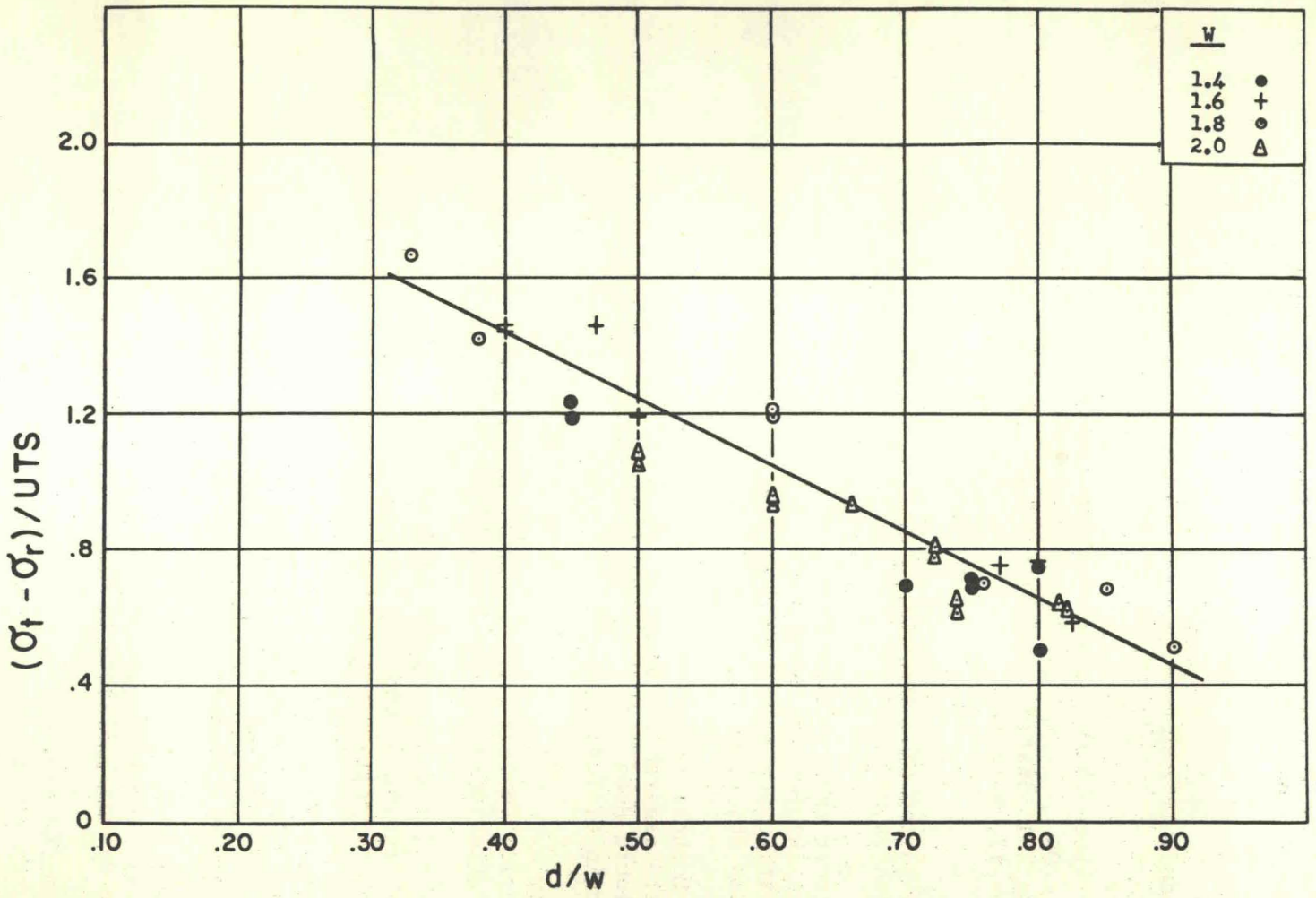

FIGURE 23. DIFFERENCE IN PRINCIPAL BORE STRESS vs RATIO OF CRACK DEPTH TO WALL THICKNESS

DISTRIBUTION LIST	Copies
Commanding General U. S. Army Weapons Command ATTN: AMSWE-CG AMSWE-RD AMSWE-OR Rock Island, Illinois	 2 4 2
Commander Armed Services Technical Information Agency ATTN: TIPDR Arlington Hall Station Arlington 12, Virginia	10
Director National Bureau of Standards Washington 25, D. C.	1
U. S. Atomic Energy Commission Technical Information Service 1901 Constitution Avenue Washington 25, D. C.	1
Applied Mechanics Reviews Southwest Research Institute 8500 Culebra Road San Antonio 6, Texas	1
Commander Air Materiel Command Wright-Patterson Air Force Base, Ohio	1
Director Ballistics Research Laboratory Aberdeen Proving Ground Aberdeen, Maryland	1
Commanding Officer U. S. Army Research Office (Durham) Box CM, Duke Station Durham, North Carolina	1
Commanding General Army Rocket & Guided Missile Agency Redstone Arsenal, Alabama	1
Commanding General White Sands Proving Grounds Las Cruces, New Mexico	1

DISTRIBUTION LIST	Copies
Commander Air Force Office of Scientific Research Air Research and Development Command ATTN: Directorate of Research Information Washington 25, D. C.	1
Chief of Naval Research Department of the Navy ATTN: Mechanics Washington 25, D. C.	1
Director U. S. Naval Research Laboratory ATTN: Mechanics Division Washington 25, D. C.	1
Chief, Bureau of Ordnance Department of the Navy ATTN: Research and Development Division Washington 25, D. C.	1
Commander Naval Ordnance Laboratory White Oak Silver Spring, Maryland	1
Commander David Taylor Model Basin Washington 7, D. C.	1
Armour Research Foundation Illinois Institute of Technology Chicago, Illinois	1
Library Massachusetts Institute of Technology Cambridge 39, Massachusetts	1
Director of Research Rensselaer Polytechnic Institute Troy, New York	1
Commanding Officer Picatinny Arsenal ATTN: Technical Information Section Dover, New Jersey	1

DISTRIBUTION LIST	Copies
Commanding Officer Detroit Arsenal Center Line, Michigan	1
Commanding Officer Watertown Arsenal Laboratories Watertown 72, Massachusetts	1
Commanding Officer Materials Research Office Watertown Arsenal Watertown 72, Massachusetts	1
Commanding Officer Diamond Fuze Laboratories ATTN: Technical Reference Section Connecticut Ave. & Van Ness St., N.W. Washington 25, D. C.	1
Commanding Officer Frankford Arsenal Philadelphia 37, Pennsylvania	1
Commanding Officer Springfield Armory Springfield, Massachusetts	1
Convair San Diego Division ATTN: Chief, Applied Research San Diego, California	1
United Aircraft Corporation Research Department 362 Main Street East Hartford 8, Connecticut	1
The Pennsylvania State University Department of Engineering Mechanics University Park, Pennsylvania	1
The General Electric Company Research Laboratories Schenectady, New York	1
Battelle Memorial Research Inst. 505 King Avenue Columbus, Ohio	1

DISTRIBUTION LIST	Copies
Director of Research Brigham Young University Provo, Utah	1
Professor of Ordnance U. S. Military Academy West Point, New York	1
Office of Technical Services ATTN: Chief, Acquisition Section Department of Commerce Washington 25, D. C.	2
Office of Technical Services Room 6814A, Main Building Department of Commerce Washington 25, D. C.	100
Director of Research California Institute of Technology Pasedena, California	1

autofrettaged cylinders up to a diameter ratio of 1.8 - 2.0 and to a much smaller degree in the non-autofrettaged condition. The rate of improvement of fatigue characteristics above 2.0 is the same for both the autofrettaged and non-autofrettaged cases.
It is shown that thermal treatment of 675°F for 6 hours after autofrettage does not affect fatigue characteristics and that there is a correlation between the cyclic stress level and the area and depth of the fatigue crack to the point of ductile rupture. The depth of the fatigue crack decreases with increasing cyclic stress level.
A means for using data from a uni-directional tensile fatigue test to predict the fatigue characteristics of thick-walled cylinders is discussed.

autofrettaged cylinders up to a diameter ratio of 1.8 - 2.0 and to a much smaller degree in the non-autofrettaged condition. The rate of improvement of fatigue characteristics above 2.0 is the same for both the autofrettaged and non-autofrettaged cases.
It is shown that thermal treatment of 675°F for 6 hours after autofrettage does not affect fatigue characteristics and that there is a correlation between the cyclic stress level and the area and depth of the fatigue crack to the point of ductile rupture. The depth of the fatigue crack decreases with increasing cyclic stress level.
A means for using data from a uni-directional tensile fatigue test to predict the fatigue characteristics of thick-walled cylinders is discussed.

autofrettaged cylinders up to a diameter ratio of 1.8 - 2.0 and to a much smaller degree in the non-autofrettaged condition. The rate of improvement of fatigue characteristics above 2.0 is the same for both the autofrettaged and non-autofrettaged cases.
It is shown that thermal treatment of 675°F for 6 hours after autofrettage does not affect fatigue characteristics and that there is a correlation between the cyclic stress level and the area and depth of the fatigue crack to the point of ductile rupture. The depth of the fatigue crack decreases with increasing cyclic stress level.
A means for using data from a uni-directional tensile fatigue test to predict the fatigue characteristics of thick-walled cylinders is discussed.

autofrettaged cylinders up to a diameter ratio of 1.8 - 2.0 and to a much smaller degree in the non-autofrettaged condition. The rate of improvement of fatigue characteristics above 2.0 is the same for both the autofrettaged and non-autofrettaged cases.
It is shown that thermal treatment of 675°F for 6 hours after autofrettage does not affect fatigue characteristics and that there is a correlation between the cyclic stress level and the area and depth of the fatigue crack to the point of ductile rupture. The depth of the fatigue crack decreases with increasing cyclic stress level.
A means for using data from a uni-directional tensile fatigue test to predict the fatigue characteristics of thick-walled cylinders is discussed.

AD Accession No.
Watervliet Arsenal, Watervliet, N. Y.

FATIGUE CHARACTERISTICS OF OPEN-END THICK-WALLED CYLINDERS UNDER CYCLIC INTERNAL PRESSURE
by T. E. Davidson, R. Eisenstadt and A. N. Reiner

Report No. WVT-RI-6216, August 1962, pages, 23 figures and 1 table.
Unclassified Report

Thick-walled cylinder fatigue data due to cyclic internal pressure for open-end cylinders in the range of 10^3 to 10^5 cycles to failure and having a diameter ratio of 1.4 to 2.0 at a nominal yield strength of 160,000 pounds per square inch is presented. Discussed and also presented are the effects of autofrettage on the fatigue characteristics of thick-walled cylinders. Autofrettage substantially enhances fatigue characteristics at stress levels below the corresponding overstrain pressure; the degree of improvement increasing with decreasing stress levels. The rate of improvement in fatigue characteristics increases significantly with diameter ratio in

(Over)

UNCLASSIFIED

Fatigue
Fracture
Gun Barrels
Pressure Vessel
Thick-Walled Cylinders

Distribution Unlimited

AD Accession No.
Watervliet Arsenal, Watervliet, N. Y.

FATIGUE CHARACTERISTICS OF OPEN-END THICK-WALLED CYLINDERS UNDER CYCLIC INTERNAL PRESSURE
by T. E. Davidson, R. Eisenstadt and A. N. Reiner

Report No. WVT-RI-6216, August 1962, pages, 23 figures and 1 table.
Unclassified Report

Thick-walled cylinder fatigue data due to cyclic internal pressure for open-end cylinders in the range of 10^3 to 10^5 cycles to failure and having a diameter ratio of 1.4 to 2.0 at a nominal yield strength of 160,000 pounds per square inch is presented. Discussed and also presented are the effects of autofrettage on the fatigue characteristics of thick-walled cylinders. Autofrettage substantially enhances fatigue characteristics at stress levels below the corresponding overstrain pressure; the degree of improvement increasing with decreasing stress levels. The rate of improvement in fatigue characteristics increases significantly with diameter ratio in

(Over)

UNCLASSIFIED

Fatigue
Fracture
Gun Barrels
Pressure Vessel
Thick-Walled Cylinders

Distribution Unlimited

AD Accession No.
Watervliet Arsenal, Watervliet, N. Y.

FATIGUE CHARACTERISTICS OF OPEN-END THICK-WALLED CYLINDERS UNDER CYCLIC INTERNAL PRESSURE
by T. E. Davidson, R. Eisenstadt and A. N. Reiner

Report No. WVT-RI-6216, August 1962, pages, 23 figures and 1 table.
Unclassified Report

Thick-walled cylinder fatigue data due to cyclic internal pressure for open-end cylinders in the range of 10^3 to 10^5 cycles to failure and having a diameter ratio of 1.4 to 2.0 at a nominal yield strength of 160,000 pounds per square inch is presented. Discussed and also presented are the effects of autofrettage on the fatigue characteristics of thick-walled cylinders. Autofrettage substantially enhances fatigue characteristics at stress levels below the corresponding overstrain pressure; the degree of improvement increasing with decreasing stress levels. The rate of improvement in fatigue characteristics increases significantly with diameter ratio in

(Over)

UNCLASSIFIED

Fatigue
Fracture
Gun Barrels
Pressure Vessel
Thick-Walled Cylinders

Distribution Unlimited

AD Accession No.
Watervliet Arsenal, Watervliet, N. Y.

FATIGUE CHARACTERISTICS OF OPEN-END THICK-WALLED CYLINDERS UNDER CYCLIC INTERNAL PRESSURE
by T. E. Davidson, R. Eisenstadt and A. N. Reiner

Report No. WVT-RI-6216, August 1962, pages, 23 figures and 1 table.
Unclassified Report

Thick-walled cylinder fatigue data due to cyclic internal pressure for open-end cylinders in the range of 10^3 to 10^5 cycles to failure and having a diameter ratio of 1.4 to 2.0 at a nominal yield strength of 160,000 pounds per square inch is presented. Discussed and also presented are the effects of autofrettage on the fatigue characteristics of thick-walled cylinders. Autofrettage substantially enhances fatigue characteristics at stress levels below the corresponding overstrain pressure; the degree of improvement increasing with decreasing stress levels. The rate of improvement in fatigue characteristics increases significantly with diameter ratio in

(Over)

UNCLASSIFIED

Fatigue
Fracture
Gun Barrels
Pressure Vessel
Thick-Walled Cylinders

Distribution Unlimited